

# A NEW APPROACH TO FIBROUS COMPOSITE LAMINATE STRENGTH PREDICTION

L. J. Hart-Smith  
©Douglas Aircraft Company  
McDonnell Douglas Corporation, 1989



N 9 2 - 3 2 5 8 8

P-31

## ABSTRACT

A new method of predicting the strength of cross-plyed fibrous composite laminates is based on expressing the classical maximum-shear-stress failure criterion for ductile metals in terms of strains. Starting with such a formulation for classical isotropic materials, the derivation is extended to orthotropic materials having a longitudinal axis of symmetry, to represent the fibers in a unidirectional composite lamina. The only modification needed to represent those same fibers with properties normalized to the lamina rather than fiber is a change in axial modulus. A mirror image is added to the strain-based "lamina" failure criterion for fiber-dominated failures to reflect the cutoffs due to the presence of orthogonal fibers. It is found that the combined failure envelope is now identical with the well-known maximum-strain failure model in the tension-tension and compression-compression quadrants but is truncated in the shear quadrants. The successive application of this simple failure model for fibers in the  $0^\circ/90^\circ$  and  $\pm 45^\circ$  orientations, in turn, is shown to be the necessary and sufficient characterization of the fiber-dominated failures of laminates made from fibers having the same tensile and compressive strengths. When one such strength is greater than the other, the failure envelope is appropriately truncated for the lesser direct strain. The shear-failure cutoffs are now based on the higher axial strain to failure since they occur at lower strains than and are usually not affected by such mechanisms as microbuckling. Premature matrix failures can also be covered by appropriately truncating the fiber failure envelope. Matrix failures are excluded from consideration for conventional fiber/polymer composites but the additional features needed for a more rigorous analysis of exotic materials are covered. The new failure envelope is compared with published biaxial test data. The theory is developed for unnotched laminates but is easily shrunk to incorporate reductions to allow for bolt holes, cutouts, reduced compressive strength after impact, and the like.

## INTRODUCTION

Failure or yield of metals has traditionally been characterized in terms of applied stresses. It makes little difference for isotropic materials whether such expressions are formulated in terms of stress or strain. However, it makes a tremendous difference in predicting failure of orthotropic materials such as fibrous composites. Indeed, the almost universal preference for a stress-based reference has handicapped failure prediction for composites for a quarter of a century. In stress formulations, it has been incorrectly assumed that the longitudinal and transverse properties of the unidirectional lamina, which have served as the basis of laminated composite analysis, are independent quantities that need to be specified separately for use in an interactive type of failure criterion.

If the formulation had been in terms of strain, the dependence between longitudinal and transverse strengths would have been apparent. The characterization of failure or yield in terms of strain rather than stress permits a single universal criterion to cover *all* materials, isotropic and orthotropic. In the

662 INDIVIDUALLY BLANK

case of fibrous composites, the current longitudinal tests (tension and compression) are sufficient to characterize correctly the fiber-dominated failures while the measured transverse strengths, which have nothing to do with the failure of the fibers, can serve as the basis of a separate failure criterion for the resin matrix.

This paper explains how failure can be characterized in terms of strain rather than stress. The conversion for isotropic materials — metal alloys, for example — is derived first to show the tie-in to established methods. The formulation in terms of strain is then extended to orthotropic materials. That nonsymmetric failure criterion for a unidirectional fibrous composite lamina is next simplified by superposition with an equivalent strength cutoff for any orthogonal layer of the *same* composite material since, for most practical structural laminates, some orthogonal fibers will always be present.

The reduced envelope is then recognizable as a truncation in the in-plane shear quadrants of the well-known maximum-strain failure model. Whenever there are orthogonal fibers present, such an envelope is not an arbitrary truncation but is directly equivalent to the generalized maximum-shear-stress failure criterion developed earlier by the author. But now it is simplified to the point where it should be more appealing to designers and, more important, it is so formulated that there is no need to specify any transverse properties. Consequently, researchers and analysts need not be skilled in the art to make realistic laminate strength predictions.

#### THE MAXIMUM-SHEAR-STRESS FAILURE CRITERION IN TERMS OF STRAIN FOR ISOTROPIC HOMOGENEOUS MATERIALS

Since the shear stresses and strains are related for isotropic materials by the simple relation

$$\tau = G\gamma \quad (1)$$

there is a one-to-one match between stress  $\tau$  and strain  $\gamma$ . The characterization of failure in terms of Mohr circles of stress and strain (Figures 1 and 2, respectively) is as follows.

For uniaxial tension, for example, failure can be expressed by the following equations.

$$\sigma_{crit} = 2\tau_{crit} \quad (2)$$

or

$$\gamma_{crit} = (1 + \nu)\epsilon_{crit} \quad (3)$$

Similarly, for pure shear, the equal and opposite orthogonal principal stresses at failure are equal to the shear strength of the material.

$$\sigma = \tau_{crit} \quad (4)$$

and

$$\epsilon = \pm \gamma_{crit}/2 \quad (5)$$

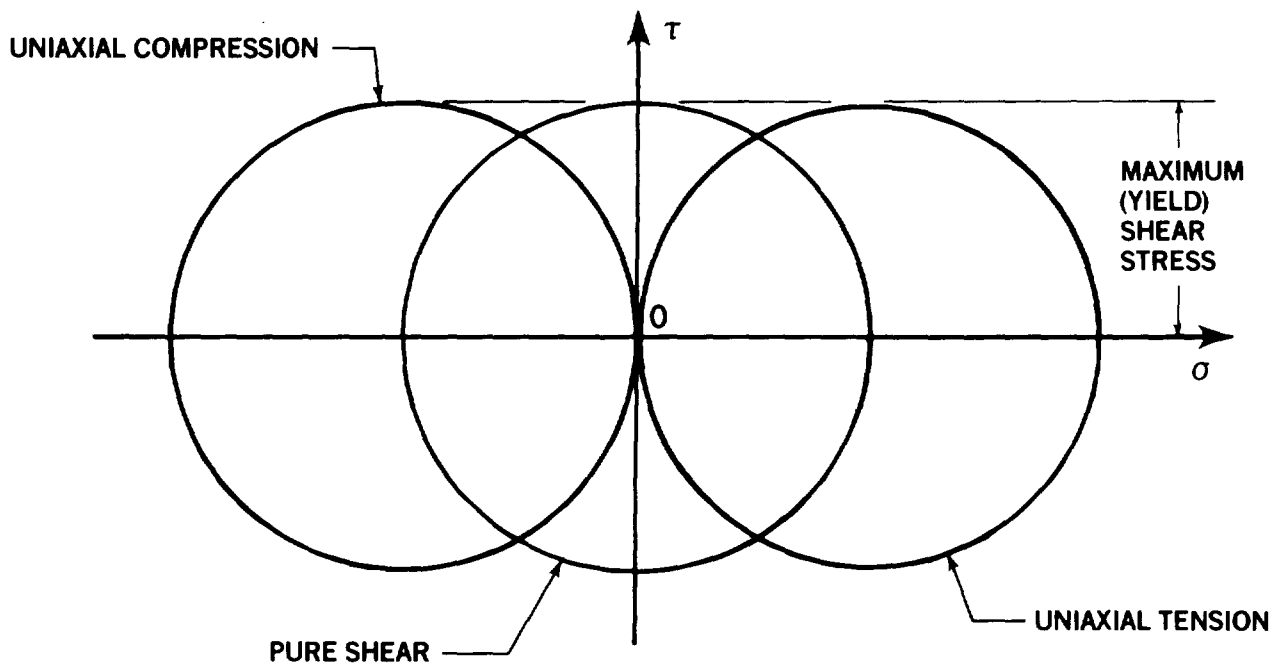


FIGURE 1. MOHR STRESS CIRCLES FOR ISOTROPIC MATERIALS

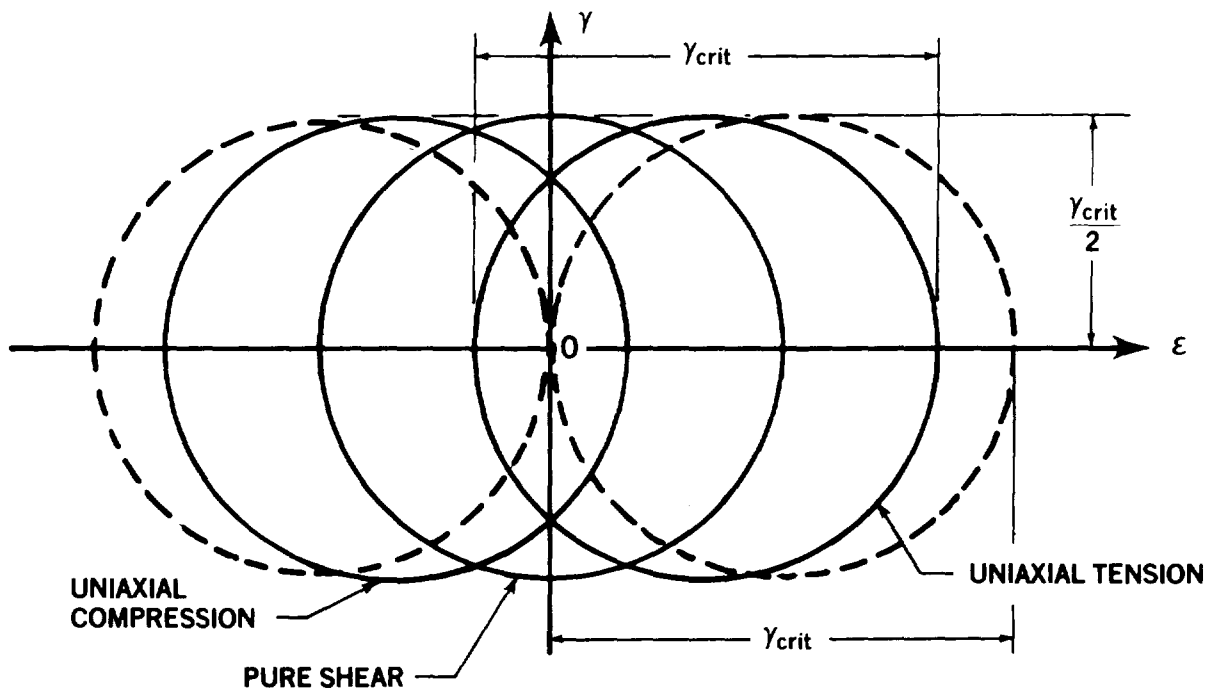


FIGURE 2. MOHR STRAIN CIRCLES FOR ISOTROPIC MATERIALS

*OH*

The general stress-strain relations for isotropic materials, using  $x$  and  $y$  as principal in-plane references and  $z$  as the thickness (normal) direction, are as follows.

$$\epsilon_x = \frac{1}{E}(\sigma_x - \nu\sigma_y - \nu\sigma_z) \quad (6)$$

$$\epsilon_y = \frac{1}{E}(-\nu\sigma_x + \sigma_y - \nu\sigma_z) \quad (7)$$

and

$$\epsilon_z = \frac{1}{E}(-\nu\sigma_x - \nu\sigma_y + \sigma_z) \quad (8)$$

Failure would occur when any of the three principal strain differentials  $(\epsilon_x - \epsilon_y)$ ,  $(\epsilon_x - \epsilon_z)$ ,  $(\epsilon_y - \epsilon_z)$ , exceeded the material allowable shear strain  $\gamma_{crit}$ . This condition is expressed in Figure 3. The figure is unbounded along the diagonal because, with triaxial (hydrostatic) stresses all having the same sign (positive or negative), the *differences* between the principal strains can remain too small to cause failure. That open-endedness can be eliminated for the special two-dimensional load case of interest here, in which there are no normal or through-the-thickness shear stresses. For this case,

$$\sigma_z = \tau_{xz} = \tau_{yz} \equiv 0 \quad (9)$$

and Equations (6) to (8) reduce to the following.

$$\epsilon_x = \frac{1}{E}(\sigma_x - \nu\sigma_y) \quad (10)$$

$$\epsilon_y = \frac{1}{E}(-\nu\sigma_x + \sigma_y) \quad (11)$$

and

$$\epsilon_z = -\frac{\nu}{E}(\sigma_x + \sigma_y) \quad (12)$$

Figure 3 represents the critical differences between the in-plane ( $x$  and  $y$ ) strains. The missing characteristics refer to the differences between the other pairs of strains. For the case  $\epsilon_x - \epsilon_z = \gamma_{crit}$ , the additional cutoffs are defined by

$$\epsilon_x = (1 - \nu)\gamma_{crit} - \nu\epsilon_y \quad (13)$$

while, for  $\epsilon_y - \epsilon_z = \gamma_{crit}$ , the remaining cutoffs (for positive and negative strains) are given as follows.

$$\epsilon_y = (1 - \nu)\gamma_{crit} - \nu\epsilon_x \quad (14)$$

Together with the cutoff  $\epsilon_x - \epsilon_y = \gamma_{crit}$  shown in Figure 3, the complete failure envelope in the absence of surface stresses is as shown in Figure 4.

Figure 5 adds to the failure envelope the traces for the uniaxial load lines  $\sigma_y = \sigma_z = 0$  and  $\sigma_x = \sigma_z = 0$ , inclined from the reference axes by an angle defined by the Poisson's ratio, as shown.

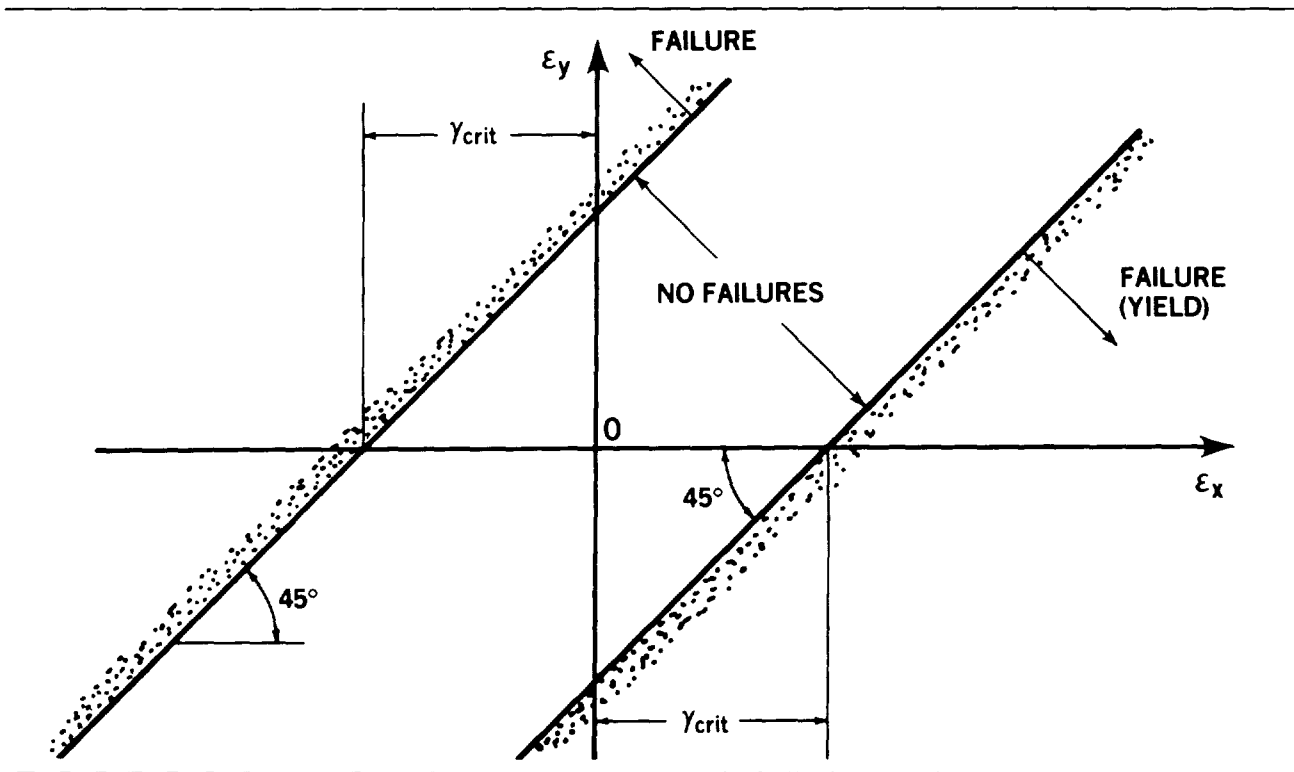


FIGURE 3. MAXIMUM-SHEAR-STRESS FAILURE CRITERION FOR ISOTROPIC MATERIALS

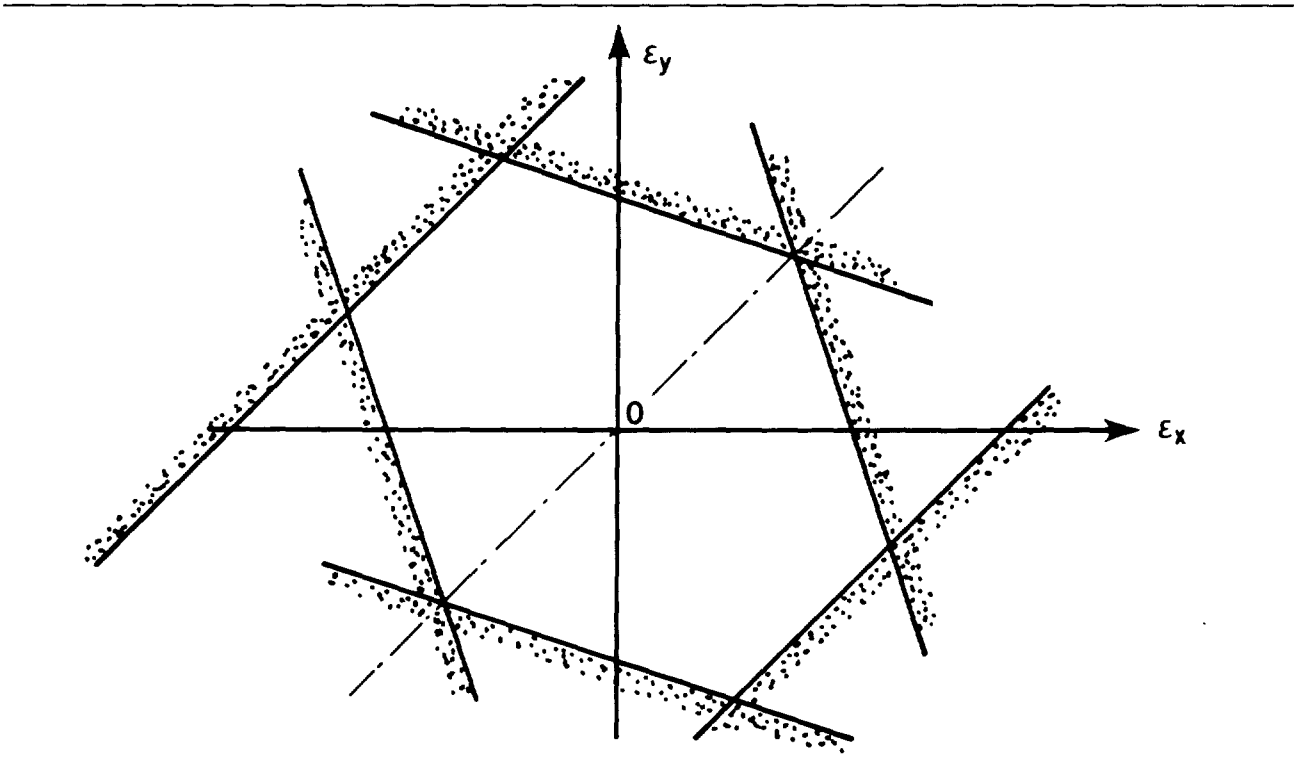


FIGURE 4. ADDITIONAL CUTOFFS DUE TO ABSENCE OF NORMAL STRESSES ( $\sigma_z = 0$ )

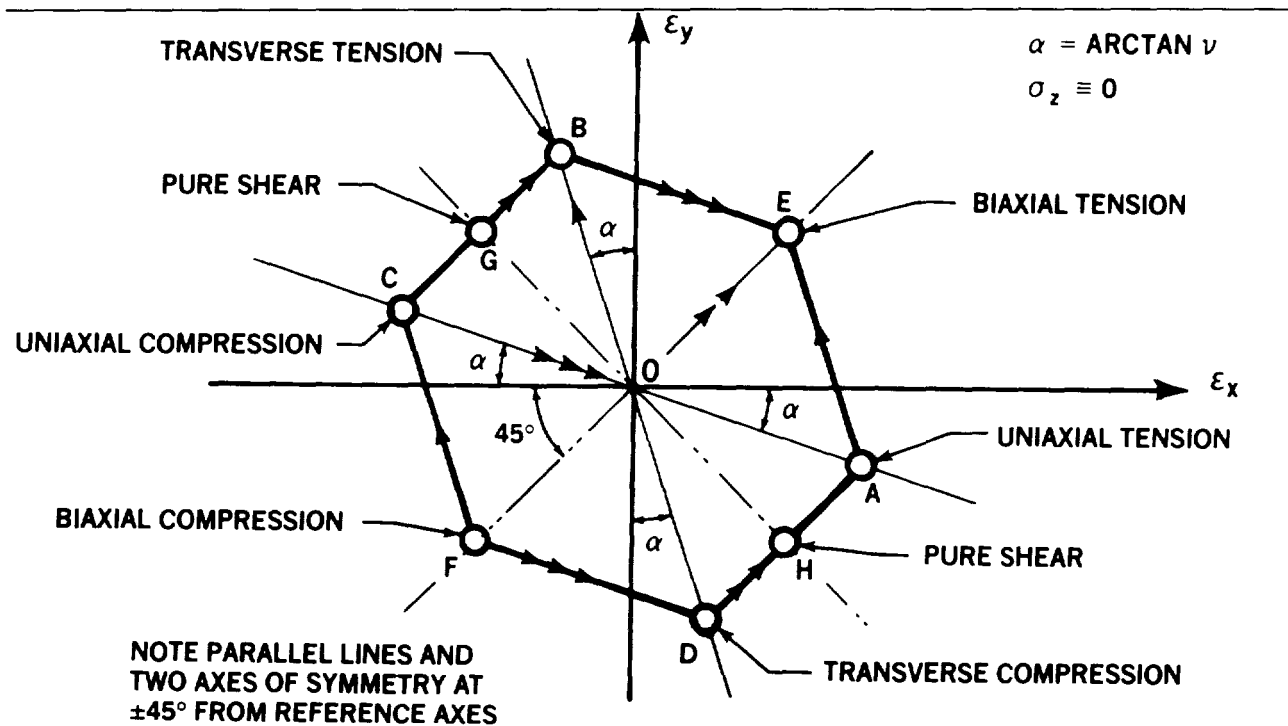


FIGURE 5. TWO-DIMENSIONAL MAXIMUM-SHEAR-STRESS FAILURE CRITERION FOR ISOTROPIC MATERIALS

These uniaxial load lines intersect the failure envelope at points A, B, C, and D. At the biaxial points E and F,  $\sigma_x = \sigma_y$  in tension and compression, respectively. G and H indicate the points of pure in-plane shear, for which  $\sigma_x = -\sigma_y$ .

All but the in-plane shear failure lines AB and CD in Figures 4 and 5 have precisely the same length and one of only two orientations, with slopes defined by the Poisson's ratio.

The uniaxial strain at failure is given by

$$\epsilon_0 = \gamma_{crit}/(1 + \nu) \tag{15}$$

and it is now apparent that the critical shear strain, or principal direct strain *difference*, is the primary quantity and that the axial strain  $\epsilon_0$  is secondary. The critical strain combination at the biaxial points is defined by

$$\epsilon_x = \epsilon_y = \left( \frac{1 - \nu}{1 + \nu} \right) \gamma_{crit} = (1 - \nu)\epsilon_0 \tag{16}$$

while the in-plane strains at the shear failure points can be seen to be as follows.

$$\epsilon_x = -\epsilon_y = \pm \gamma_{crit}/2 = \pm (1 + \nu)\epsilon_0/2 \tag{17}$$

Before generating equivalent failure criteria for orthotropic materials, it is useful to interpret some of the less obvious lines in Figure 5. The radial lines OA, OB, OC, and OD are easily interpreted as uniaxial load lines. At point A,  $\sigma_y = \sigma_z = 0$  and  $\sigma_x \neq 0$ . Along the line AE, the stress  $\sigma_y$  is increased in

such a way that the stress *difference*  $\sigma_x - \sigma_z$  is held constant because the application of  $\sigma_y$  stresses cannot possibly induce any stresses in the  $x - z$  plane — only compatible Poisson strains. Therefore, the axial and normal strains  $\epsilon_x$  and  $\epsilon_z$  must decrease by an amount  $\nu\epsilon_y$  as  $\sigma_y$  increases. Since  $\sigma_z$  is zero at point A,  $\sigma_x$  is constant all along the lines AE and DF. The normal stress  $\sigma_z$  is zero throughout Figure 5, so the stress difference  $\sigma_x - \sigma_z$  is also constant along the lines AE and DF. Similarly,  $\sigma_y$  is constant along the lines CE and BF.

The lengths of all the sides of the hexagon in Figures 4 and 5 would be identical only for one particular value of the Poisson's ratio. That value is obtained by equating the lengths of the usually different sides, as in the following equation.

$$\frac{\sqrt{(1 + \nu^2)}}{(1 + \nu)} = \sqrt{2} \left( \frac{1 - \nu}{1 + \nu} \right)$$

$$(1 + \nu^2) = 2(1 - 2\nu + \nu^2)$$

or

$$1 - 4\nu + \nu^2 = 0 \tag{18}$$

The result,  $\nu = 0.2679$  is typical for metals, so that the sides of most hexagons would be nearly equal.

#### **THE (ISOTROPIC) MAXIMUM-SHEAR-STRESS FAILURE CRITERION FORMULATED IN TERMS OF STRAINS FOR ORTHOTROPIC LAMINAE**

The next step is to generalize the preceding analysis to orthotropic layers. The failure criterion to be derived should actually refer to the fiber, for fiber-dominated failures, *not* the lamina. However, the fibers and matrix obviously share a common strain along the fiber axis. For the usual case, in which strong, stiff fibers are embedded in a soft matrix, it is possible to bypass the micromechanical calculations relating the transverse strains of the fiber to those of the lamina because of the greater criticality of the fiber failure criterion. Such a simplification may not be realistic for some of the more exotic advanced composites, and a more comprehensive theory would be needed then.

It is assumed again that there are no normal or through-the-thickness shear stresses acting on the laminate. Using the subscripts  $L$ ,  $T$ , and  $N$  to denote the longitudinal, transverse (in-plane), and normal directions, respectively, Equations (10) to (12) can be generalized for transversely isotropic materials to read as follows when the axis of symmetry is longitudinal.

$$\epsilon_L = \frac{1}{E_L}(\sigma_L - \nu_{LT}\sigma_T) \tag{19}$$

$$\epsilon_T = \frac{1}{E_T}(\sigma_T - \nu_{TL}\sigma_L) = -\nu_{LT}\sigma_L/E_L + \sigma_T/E_T \tag{20}$$

and

$$\epsilon_N = \frac{1}{E_T}(-\nu_{TL}\sigma_L - \nu_{TN}\sigma_T) \tag{21}$$

For a uniaxial load along the fibers, with neither lateral nor normal applied stress, the axial strain in both the fiber and lamina will be  $\epsilon_0$  at failure and the associated lateral and normal strains will be

$-\nu_{LT} \epsilon_0$  in the *lamina*. The corresponding orthogonal strain in the *fiber*, which can be presumed to have a different Poisson's ratio from the homogenized lamina, is undefined. However, for typical carbon-epoxy composites, the similarity of the Poisson's ratio  $\nu_{LT}$  for the unidirectional lamina and for an isotropic resin matrix, implies that the corresponding Poisson's ratio for the fiber must also be similar. If a substantial difference is expected between the Poisson's ratios for the fiber and monolayer, one would need to complete the micromechanical analyses relating the two before proceeding with the formulation of the failure criteria. And the appropriate distinction would need to be made for all states of stress being considered.

Figure 6 shows the traces of these uniaxial load lines, in tension and compression, on the  $\epsilon_L - \epsilon_T$  in-plane strain plane. If the tension and compression strengths are the same, it is possible to locate the 45-degree sloping shear-failure lines on which the uniaxial failures are represented by individual points. If the tensile and compressive strengths differ, the numerically greater value defines both shear-failure lines, as shown in Figure 6, while the lesser strength defines a cutoff due to some other failure mechanism, such as microbuckling under compression.

For a uniaxial in-plane load perpendicular to the fibers, a different Poisson's ratio,  $\nu_{TL}$ , is involved and the uniaxial load line is no longer symmetric as it was for isotropic materials in Figure 4. The traces of this unidirectional load condition can be added to Figure 6, and wherever they cross the shear-failure lines denotes the points of failure of the *fibers*.\*

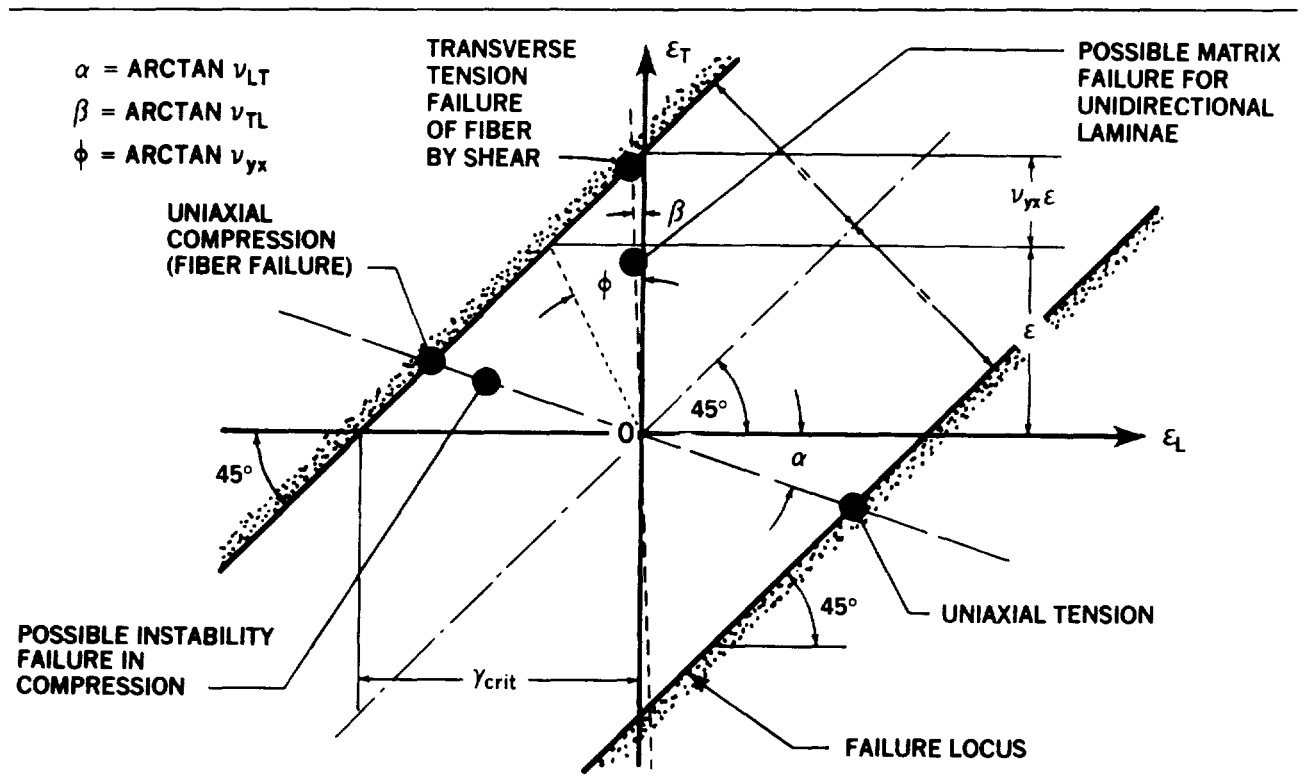


FIGURE 6. SHEAR FAILURE LOCI FOR ORTHOTROPIC MATERIALS

\* With unidirectional laminae, the matrix may fail prematurely under transverse tension at a lower strain, but that is normally suppressed for any typical cross-plyed structural laminate and may be considered as a special case.



It is apparent that the same critical shear strain holds throughout the entire region of interest in Figure 6 since the sum of longitudinal and orthogonal strains is always

$$\epsilon_0 + \nu\epsilon_0 = \gamma_{crit} \quad (22)$$

no matter what the value of the Poisson's ratio  $\nu$  for any particular cross-plyed laminate.

To complete Figure 6, and make it equivalent to Figure 5, constant-stress lines are added through the uniaxial stress points associated with shear failures of the fibers. Or, if there are premature failures under other modes, the additional lines must be placed where the missing shear failures would have occurred. Consider, for example (Figure 6) the addition of transverse stress to the point of uniaxial tension loading, while holding the longitudinal stress in the fibers and lamina constant without altering the stress-free state in the normal direction. Doing so would require that the additional strains be in the same relation as those following the purely transverse tension line in Figure 6. Along that line, with a slope defined by  $\nu_{TL}$ , only the transverse stress varies. There are no incremental longitudinal and normal stresses, so no shear stress can be induced in the  $L-N$  plane. Likewise, the missing line from the transverse tension to the biaxial tension points must be parallel to the original longitudinal tension line in Figure 6. The entire envelope is shown completed in Figure 7 for the special case in which the tensile and compressive strengths of the unidirectional laminae are equal. Unlike Figures 4 and 5, which are

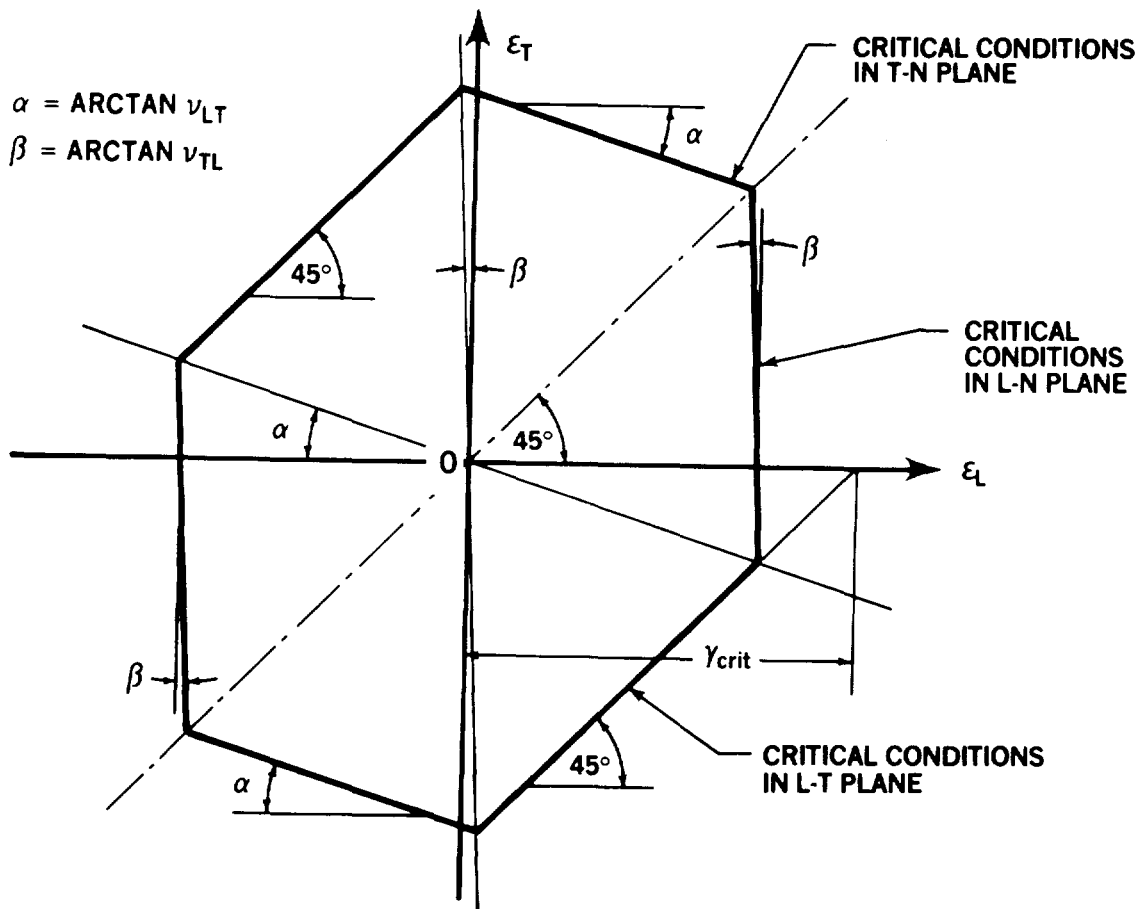
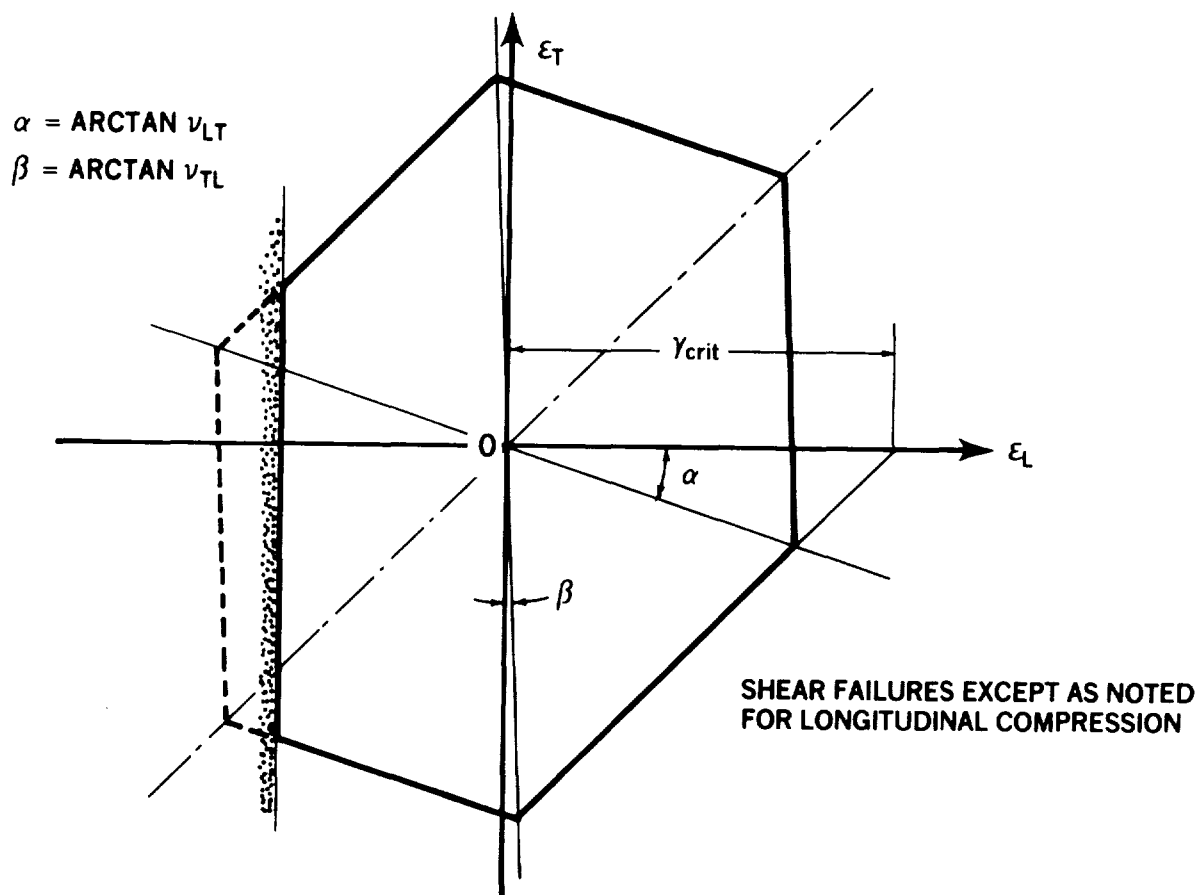


FIGURE 7. SHEAR FAILURE ENVELOPE FOR ORTHOTROPIC MATERIALS HAVING EQUAL TENSILE AND COMPRESSIVE STRENGTHS

doubly symmetric, Figure 7 is skewed because of the difference between the two in-plane Poisson's ratios. The third Poisson's ratio is involved in establishing the compatible normal strains, but does not appear in the in-plane failure envelope shown in Figure 7.

Figures 8 and 9 show the effect of fiber-dominated cutoffs at either end of the failure envelope. The cutoff representing microbuckling of the new (small-diameter) high-strain carbon fibers is drawn perpendicular to the strain axes because compression buckling is not usually sensitive to orthogonal stresses. The other cutoff, representing a lower tensile than compressive strength, is drawn parallel to the unidirectional load line since it is more likely to be a stress-imposed limit than not.



**FIGURE 8. FAILURE ENVELOPE FOR ORTHOTROPIC MATERIALS WHICH ARE STRONGER IN TENSION THAN IN COMPRESSION**

Figure 10 shows a postulated cutoff for matrix-dominated transverse tension failures. Since this would appear to be a stress rather than strain limit, the cutoff is drawn parallel to the constant transverse stress line on the basis that any longitudinal load would not induce any stress in the  $T-N$  plane.

Figures 7 through 9 refer to a fiber-dominated unidirectional lamina and could be used directly as a ply-by-ply failure criterion for analyzing cross-plyed structural laminates. However, many simplifications ensue from reinterpreting this criterion in the context of laminates *before* it is used as a strength check, as discussed in the next section.

SHEAR FAILURES EXCEPT AS NOTED  
FOR LONGITUDINAL TENSION

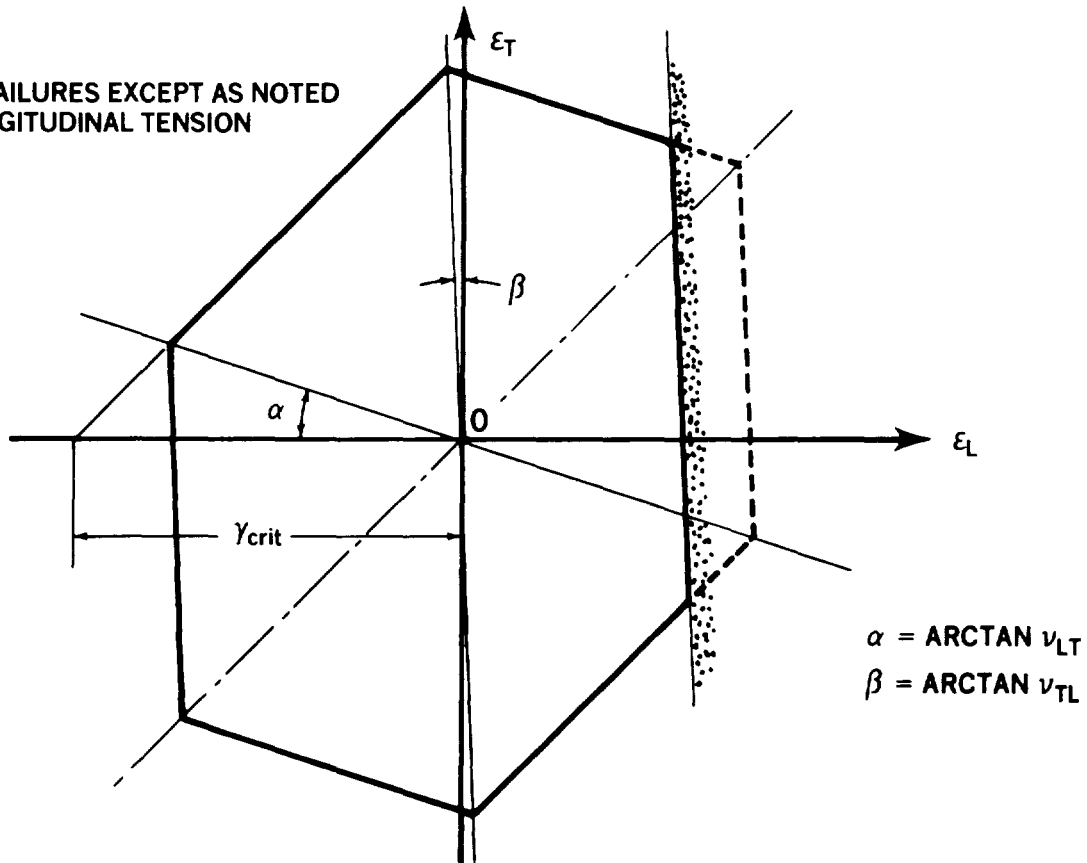
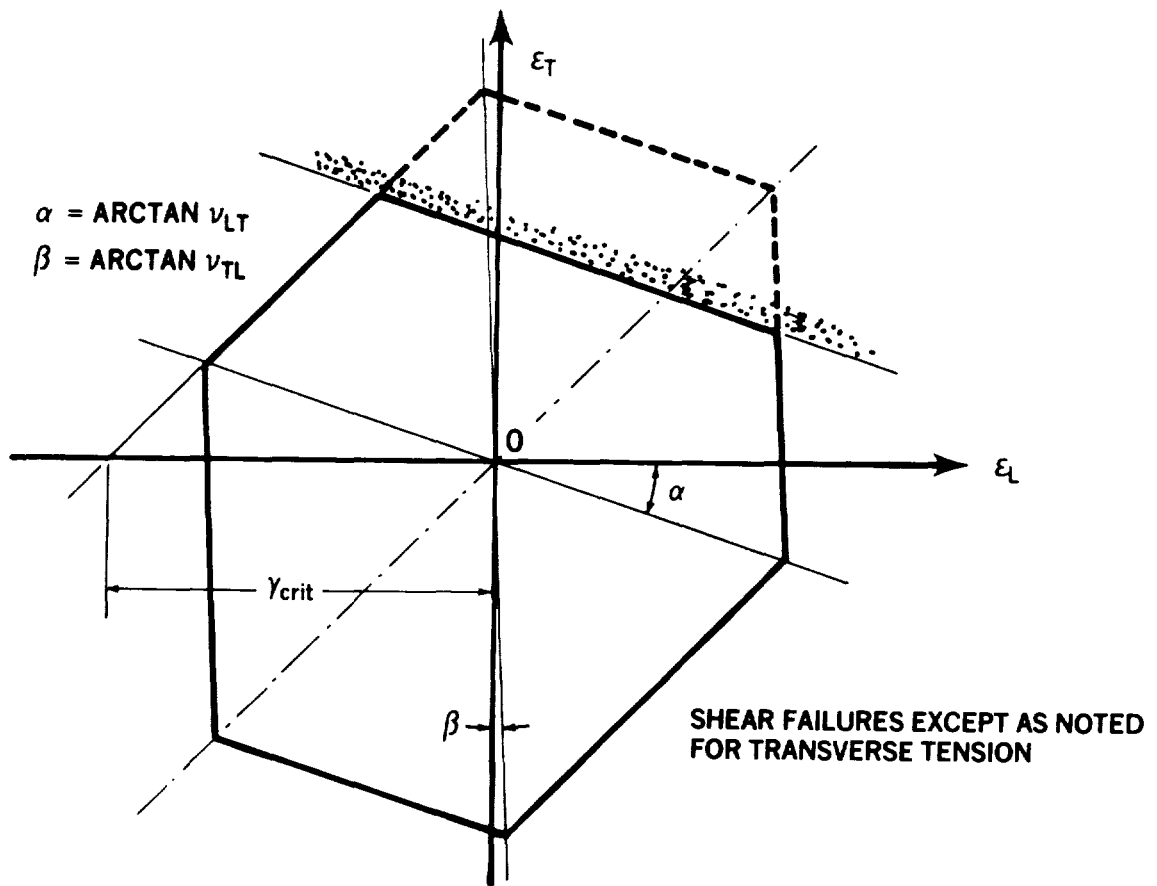


FIGURE 9. FAILURE ENVELOPE FOR ORTHOTROPIC MATERIALS WHICH ARE STRONGER IN COMPRESSION THAN IN TENSION

### THE "MAXIMUM-SHEAR-STRAIN" FAILURE CRITERION FORMULATED FOR CROSS-PLIED STRUCTURAL LAMINATES

It is now apparent that the generalization of the classical maximum-shear-stress failure criterion for ductile metals is actually most conveniently expressed as a maximum-shear-strain criterion for orthotropic materials, encompassing the classical hypothesis as a special case. Care is needed to exclude shear strains caused by factors other than stress: as, for example, by nonuniform thermal expansion or swelling due to absorbing moisture. Even when attention is paid only to the mechanically caused shear strains, there are still some difficulties since some of the Poisson-induced strains have no corresponding stresses, as discussed in the next section.

In design of composite aircraft structures, it is customary to have a minimum percentage of fibers in *all* of the four standard directions — 0°, +45°, 90°, and -45°. That being the case, the greater strains in Figures 7 through 9 in the transverse rather than longitudinal direction would be truncated by longitudinal failures in orthogonal plies. So, if there were really orthogonal plies for each fiber direction, these figures could be simplified with no loss of accuracy. This has been done in Figure 11 by adding a mirror image to Figure 7 about the biaxial strain diagonal axis and taking the smaller strength cutoffs for each segment of the envelope. The new figure is doubly symmetric, just as Figures 4 and 5 were for isotropic materials. More importantly, the corner points are defined by the Poisson's ratios for the



**FIGURE 10. FAILURE ENVELOPE FOR ORTHOTROPIC MATERIALS WHICH HAVE A WEAKNESS IN TRANSVERSE TENSION**

unidirectional laminae on which the failure envelope is based. This is of vital importance because, as shown below, those corner points remain fixed for *all* cross-plyed laminates, regardless of the Poisson's ratios of the actual laminate.

Because Figure 11 is drawn in strain space rather than stress space, it remains doubly symmetric even if the percentages of  $0^\circ$  and  $90^\circ$  fibers are *not* the same. The two laminate Poisson's ratios  $\nu_{xy}$  and  $\nu_{yx}$  would vary with the proportion of  $0^\circ$  and  $90^\circ$  fibers, but the failure envelope would *not* do so.

Consider the case of a laminate containing equal percentages of  $0^\circ$  and  $90^\circ$  fibers, with no  $\pm 45^\circ$  fibers, for which both in-plane Poisson's ratios are approximately 0.05. Figure 12 shows where the uniaxial load lines in the longitudinal and transverse directions would intersect the failure envelope in Figure 11. No intersections fall on the 45-degree sloping shear-failure lines, and the associated maximum shear strain  $(1 + \nu_{yx})\epsilon_0$  appears insufficient to have caused failure.

The explanation of this apparent anomaly is that failure is actually caused by the stress states in the planes perpendicular to the fibers, involving the normal rather than in-plane direction. A longitudinally stretched all- $0^\circ$  laminate contracts as much laterally as it does through the thickness. However, the presence of the orthogonal in-plane fibers in the  $0^\circ/90^\circ$  laminate restricts the in-plane lateral contraction, and hence the in-plane shear stress developed in both the lamina and fiber, so that this

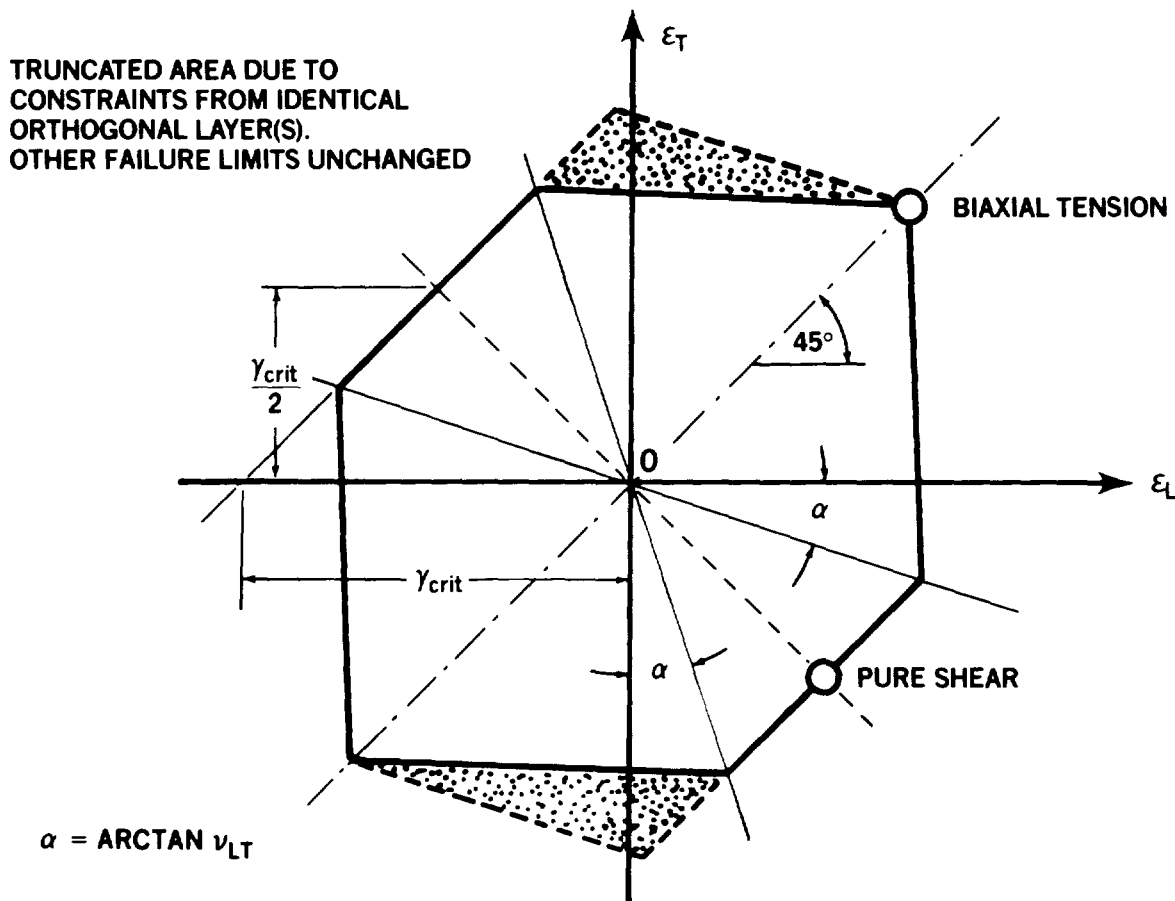


FIGURE 11. SUPERIMPOSED FAILURE ENVELOPES FOR ORTHOGONAL LAYERS OF ORTHOTROPIC MATERIALS

plane becomes less critical than the one defined by the fiber axis and the normal direction. Failure is still predicted to occur on the diagonal shear failure line in Figure 6, only now the failure point is located on Figure 12 by a radial line with a slope defined by  $\nu_{LT}$  rather than by  $\nu_{xy}$ . This is generally true for all laminate patterns for which  $\nu_{xy} > \nu_{LT}$  for the unidirectional lamina on which Figure 6 is based.

What is happening may better be understood by drawing the appropriate Mohr circles, as has been done in Figure 13. Yet, for all practical purposes, the lines with slopes defined by  $\nu_{yx}$  in Figure 12 and  $\nu_{xy}$  (not shown) also correctly identified the failure strains  $\epsilon_0$  for the  $0^\circ/90^\circ$  laminate. Similarly, the biaxial failure strains, which obviously are not associated with in-plane shear strains, are also correctly located.

If, for this same  $0^\circ/90^\circ$  laminate, biaxial rather than uniaxial loads were to be applied, one could easily envisage a little transverse compression combined with a predominantly longitudinal tension load so that the transverse strains were made to coincide with those developed by a uniaxial load on a unidirectional lamina. In such a case, failure would occur precisely on the corner point in Figure 7 because those would be the applied strains in the laminate, only they would have been developed partly by orthogonal loads instead of entirely by Poisson contractions.

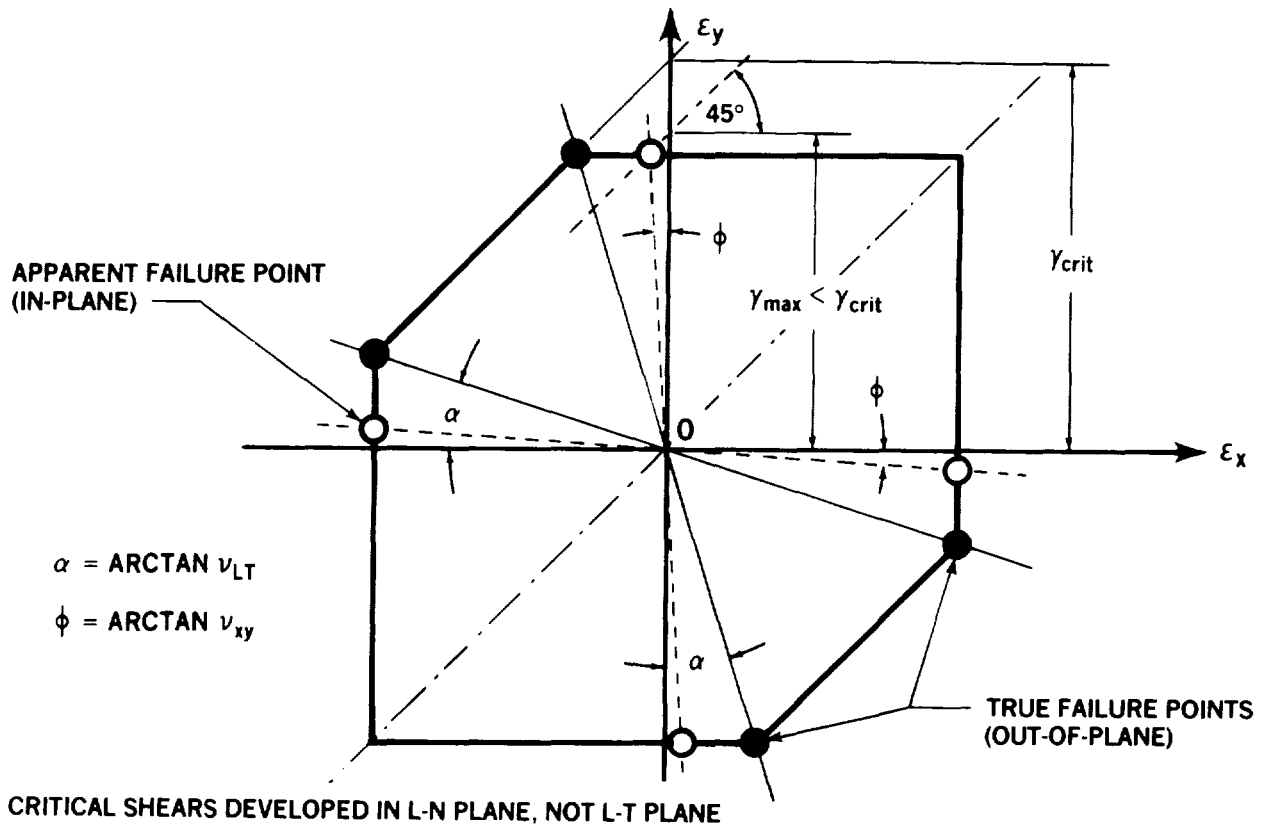
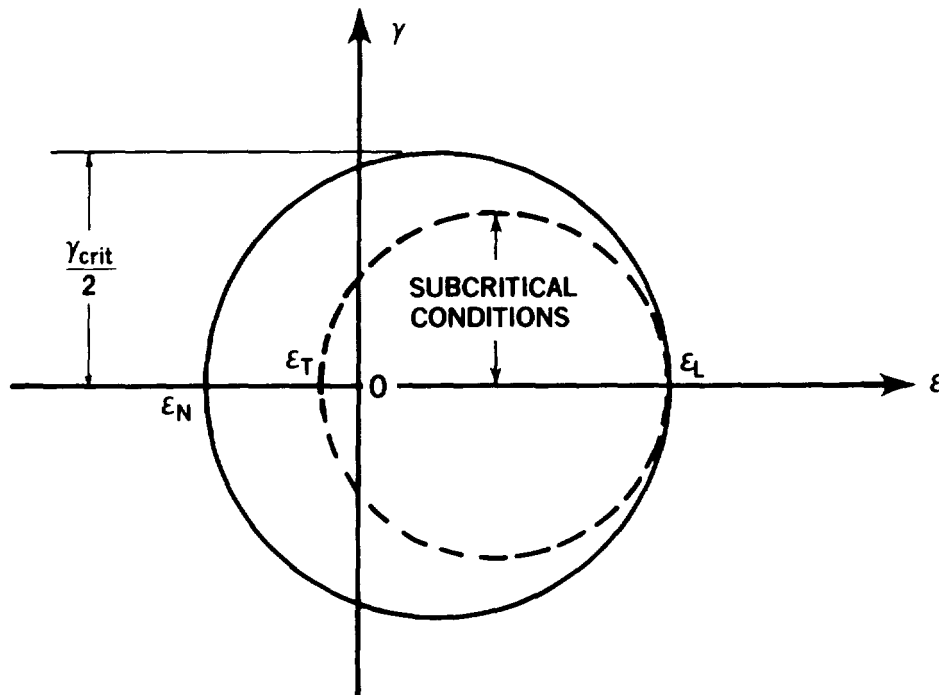


FIGURE 12. UNIAXIAL FAILURE POINTS FOR 0°/90° CROSS-PLYED LAMINATES WITH LOW POISSON'S RATIOS

Likewise, one could apply equal and opposite loads in the 0° and 90° fibers. This would induce equal and opposite strains, and failure would be predicted to occur at an axial strain of  $\gamma_{crit}/2$ , as noted in Figure 11. Indeed, that is the point where *all* purely in-plane-shear failures will occur, regardless of the particular Poisson's ratios for any particular cross-plyed laminate.

Consider next a nonstructural cross-plyed laminate consisting of 33 percent of the fibers in the 0° direction, and the remaining 67 percent shared equally between the  $\pm 45^\circ$  directions. For this laminate, the Poisson's ratio  $\nu_{xy}$  will be about 0.67, much higher than the typically 0.25 for a unidirectional lamina and the 0.33 for a quasi-isotropic laminate. In the absence of 90° fibers, one should ideally draw the unidirectional load lines on Figure 7 rather than Figure 11. The other Poisson's ratio  $\nu_{yx}$  should be about 0.2. Figure 14 shows these radial uniaxial load lines added to Figure 7. It is significant that, in the longitudinal direction, the shear-failure line is intercepted at a *lower* axial strain than was the case for the unidirectional lamina. The critical difference between strains does occur *in-plane* in this case and the longitudinal strain at failure is expected to be less than that of the unidirectional lamina in the following ratio:

$$\epsilon_{laminate} = \epsilon_{lamina} \times (1 + \nu_{LT}) / (1 + \nu_{xy}) \quad (23)$$



**FIGURE 13. EXPLANATION OF APPARENT PREMATURE FAILURE PREDICTION**

In this case, the reduction is to only 75 percent of the nominal value. Thus, this laminate without any  $90^\circ$  fibers is not only impractical because of its disproportionately small transverse ( $90^\circ$ ) strength and stiffness, but also because it does not allow the load-carrying  $0^\circ$  fibers to work to their full extent.

Actually, the loss of efficiency is probably overestimated slightly because no distinction has been made between the lateral strains in the fiber and the lamina. With a truly soft matrix, the fibers would not compress quite as much as the lamina would shrink; with a lower lateral strain experienced by the fibers, the appropriate values of transverse stress would need to be reduced. Doing so would violate the standard assumption that plane sections remain plane throughout the laminate. The maximum-strain failure model for composites may be looked upon as an overcorrection for this problem inasmuch as no allowance is made for any loss of fiber strength caused by a lateral stress of the opposite sign to the axial stress in the fiber. This issue can be resolved only by micromechanics; the same problem also exists with all the pseudo-scientific laminate strength theories.

For a quasi-isotropic laminate, the strain to failure would be predicted by Equation (23) as 94 percent of that of the unidirectional lamina. Again, in reality it would be slightly higher but, with good test specimens and test technique, it should be possible to detect a statistically significant small reduction from the unidirectional value.

If one were to test a cross-ply laminate that had the *same* Poisson's ratios as the unidirectional lamina because of the particular mixture of  $90^\circ$  and  $\pm 45^\circ$  fibers, the longitudinal strains to failure would logically be identical and the unidirectional load lines would be the same as in Figure 7.

Now, even though Figure 11 can be applied to woven fabric laminates as well as to cross-ply tape ones, the Poisson's ratios defining the corner points *must* be those of the *unidirectional* lamina, which

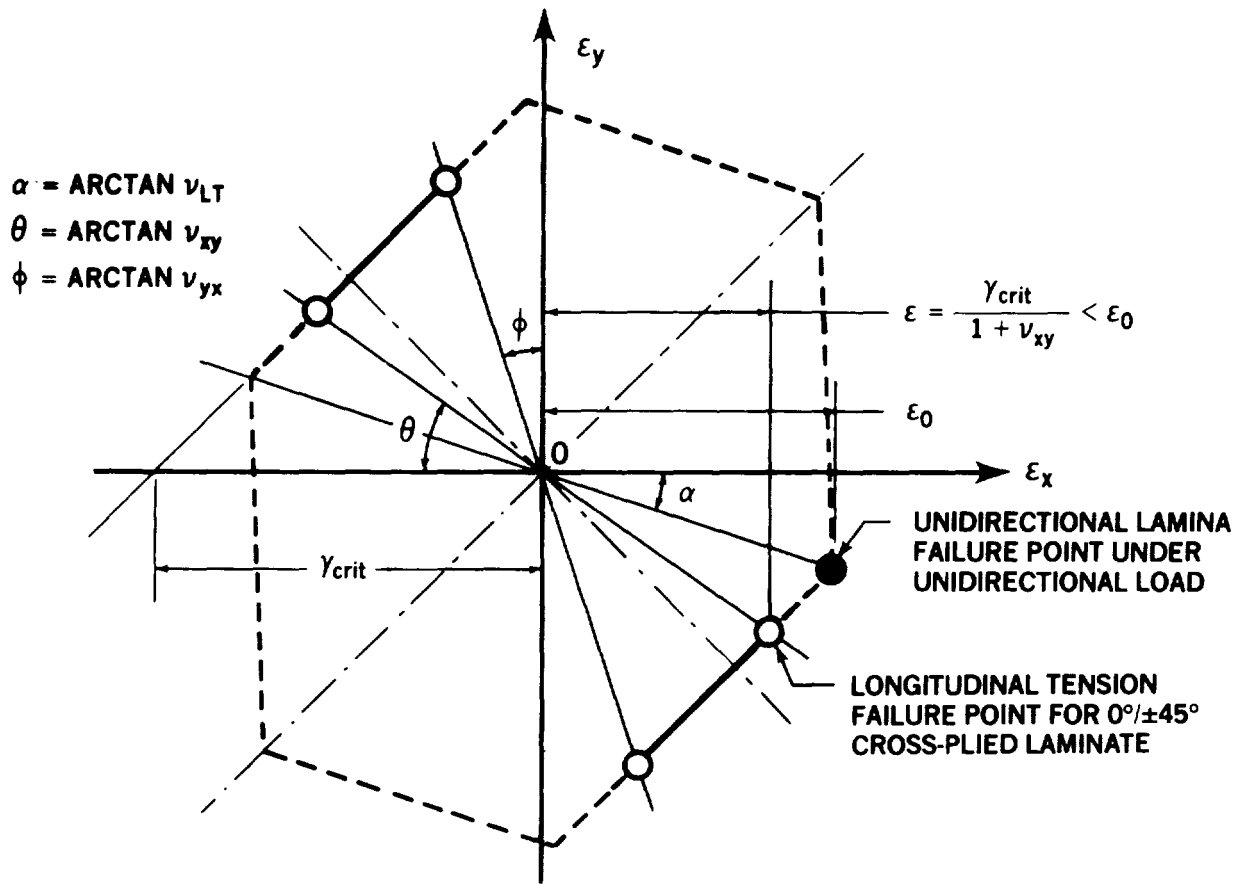


**FIGURE 14. UNIAXIAL FAILURE POINTS FOR  $0^\circ/\pm 45^\circ$  LAMINATES WITH HIGH POISSON'S RATIOS**

may be difficult to measure on a woven fabric. However, they can be easily related and the required values can be deduced reliably from measurements of the Poisson's ratio of a  $\pm 45^\circ$  woven laminate. (The direct use of the  $0^\circ/90^\circ$  laminate is not recommended for this purpose since its Poisson's ratio is so small as to be difficult to measure.)

The failure envelopes in Figures 7 through 9 would be applied, in turn, to the  $0^\circ/90^\circ$  combination of fibers and the  $\pm 45^\circ$  set. This would be necessary and sufficient to assess the strength of such laminates for fiber-dominated failures of in-plane loads. These are not unreasonable limitations since resin matrices are traditionally so weak that designers should always avoid applying direct transverse shear loads. Also, normal pressure loads must always be small in comparison with the in-plane stresses for any thin-shelled structures, although such might not be the case for deep submersible vehicles. Further, if the matrix is so weak as to prevent the fibers from developing their full strengths before failure of the laminate under in-plane loads, the matrix or the fiber pattern should be changed rather than the analysis method.

### THE TRUNCATED MAXIMUM-STRAIN FAILURE MODEL

The transverse monolayer Poisson's ratio  $\nu_{TL}$  is only about 0.025 for the usual case of carbon, boron, or glass fibers embedded in polymeric matrices like epoxies, polyester, and phenolics. It is not



unreasonable under such circumstances to approximate the almost horizontal and vertical lines joining the uniaxial and biaxial load points in Figure 11 by exactly horizontal and vertical lines, as in Figure 15. If that is done, the new failure criterion appears as a close approximation of the now classical maximum-strain failure model for fibrous composites (see Reference 1), but with the latter's over-estimated strengths in the shear quadrants eliminated. A sample of these unconservative predictions is presented in Figure 16.

$$\alpha = \text{ARCTAN } \nu_{LT} \text{ FOR UNIDIRECTIONAL LAMINA}$$

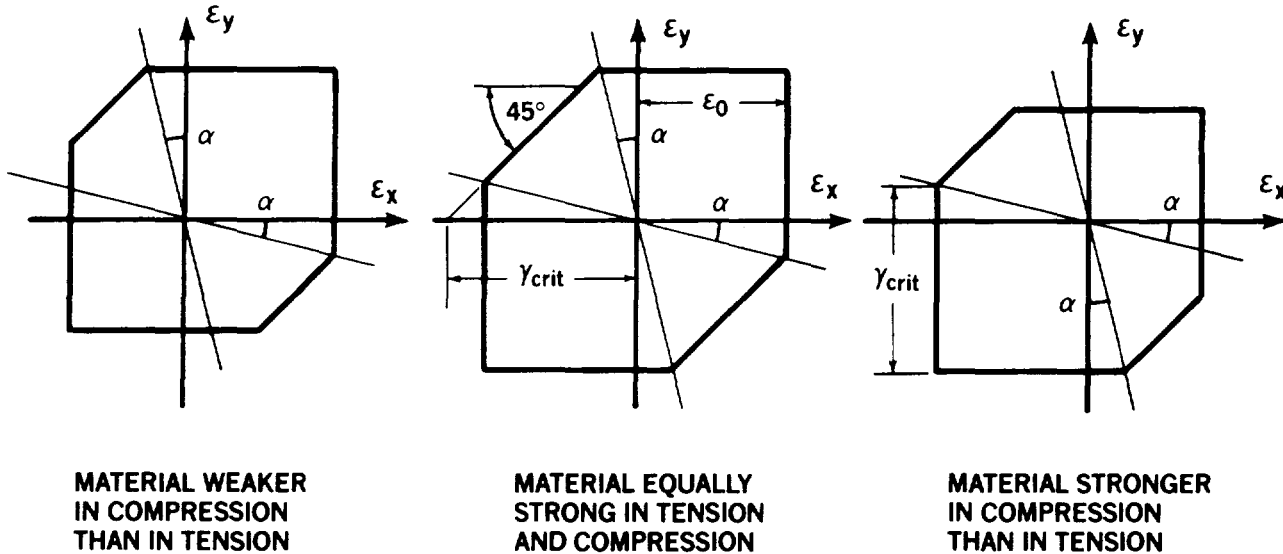


**FIGURE 15. TRUNCATED MAXIMUM-STRAIN FAILURE MODELS FOR FIBER-DOMINATED FAILURES OF CROSS-PLYED COMPOSITE LAMINATES**

Obviously, this type of simplification should not be expected to be valid for such composites as whisker-reinforced metal matrices for which the assumption of strong and stiff fibers and a soft and weak matrix would no longer be valid. But many of the structural applications of fiber/polymer composites would be well characterized by the simple failure models shown in Figure 15. Basing the application of the new failure criterion — that of the generalized maximum-shear-stress recommended by the author in References 2 through 4 — on an improvement in the well-known maximum-strain model for analyzing composite structures should have the effect of making the physics of the phenomena easier to understand. And, since it is now seen to be directly equivalent to the truly classical ductile-yield failure theory for metals, few designers and analysts should feel the kinds of insecurity and concern that have been associated with earlier composite failure criteria.

Nevertheless, the author again cautions that until a proper two-phase failure theory is developed to characterize the in situ strengths of the fibers and matrix separately, even this theory is capable of misapplication. It is unlikely to be improved upon for general-purpose analyses of today's fiber-reinforced polymer matrices, except for Kevlar (aramid) fibers that exhibit more than the two modes of failures observed in carbon fibers, so long as designs are confined within the outer shaded area in Figure 17. However, matrix failures prevail outside that area and *no* failure analyses are currently available for matrix-dominated failures of cross-plyed laminates. The problem is that this new theory, like all prior theories, is capable of being misapplied without any restrictions on permissible fiber patterns, and without warning the user that he should not believe the predictions. This problem is critical

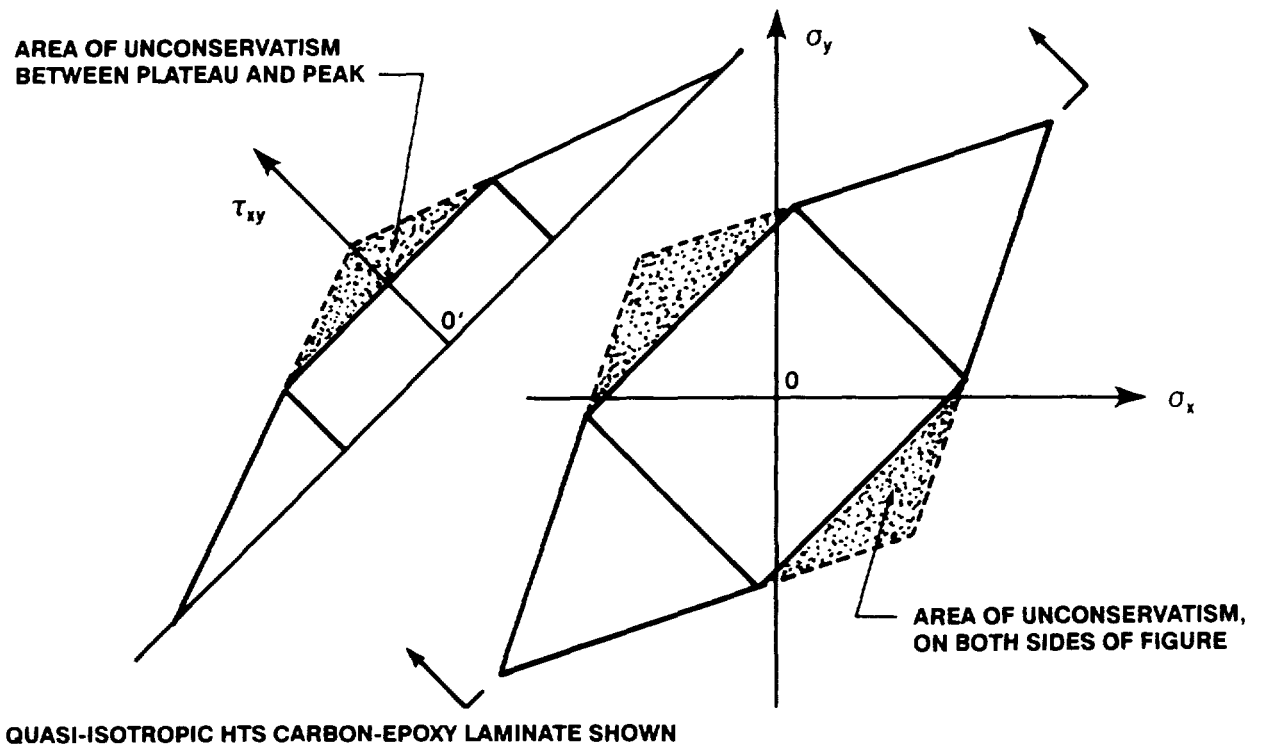
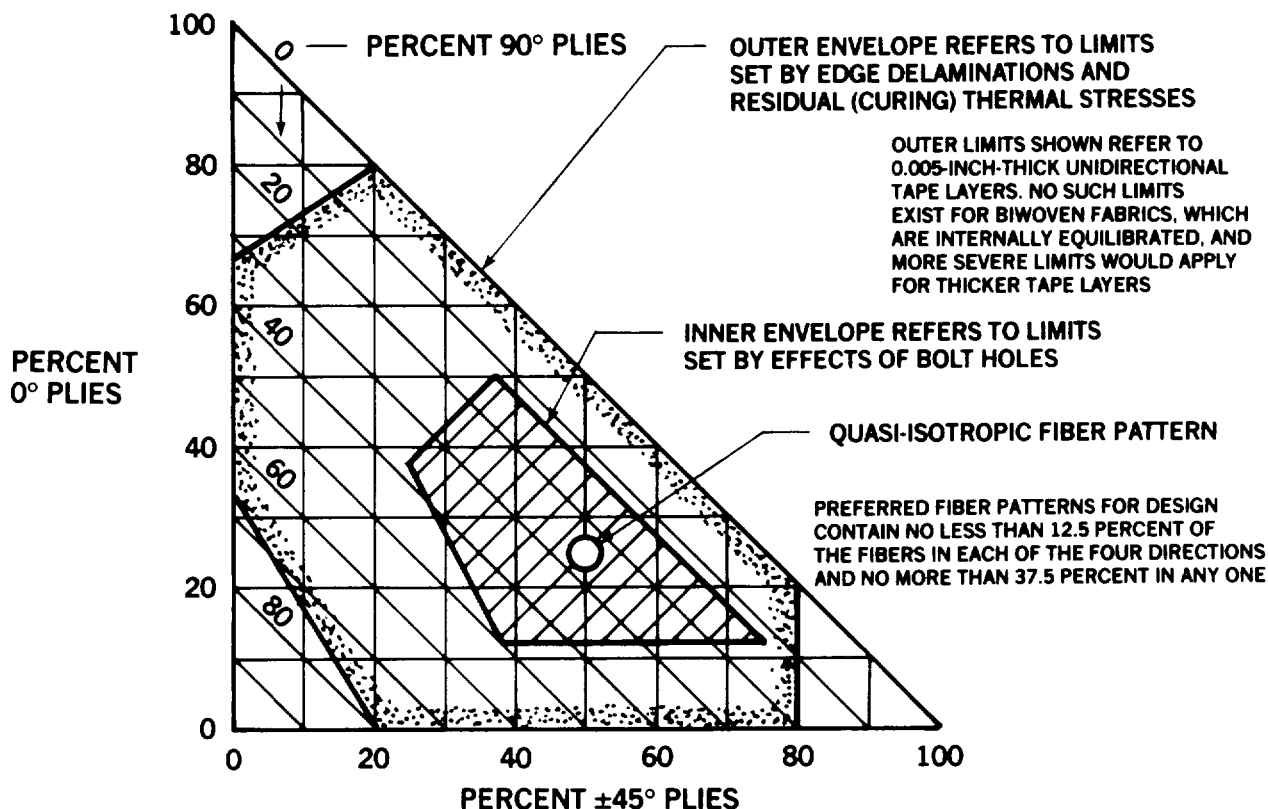


FIGURE 16. UNCONSERVATISM OF UNTRUNCATED MAXIMUM-STRAIN FAILURE MODEL

for laminate selection by computer optimization codes which are not programmed to reduce the laminate strengths for matrix-dominated failures, merely because no one has derived the necessary equations.

Ironically, a better theory for state-of-the-art fiber/polymer composites should merely discourage the use of impractical fiber patterns that have already been identified on the basis of accumulated experience but are still very much in vogue because oversimplified analyses have failed to condemn them. A better theory should not be expected to improve the strengths predicted for practical fiber patterns. However, the author believes that such improvements, from the derivation of a truly two-phase theory with possibly interface failures as well, will be vital to the use of the more exotic composites on which research has already begun.

In comparison with the "generalized maximum-shear-stress" failure criterion coded in the BLACK-ART computer program (see Reference 4), the new strain-based formulation will predict the *same* composite laminate strengths whenever input data for BLACKART have been appropriately selected to make them represent the behavior of the unidirectional lamina within a cross-plyed laminate, rather than in the isolated circumstances in which it has customarily been tested. The real beauty of the present strain-based formulation is that there is no opportunity to enter transverse properties that are incompatible with the longitudinal properties. The only data needed are the lamina effective strain-to-failure in tension and compression and the Poisson's ratios of the lamina and laminate. Conversion to the corresponding strengths requires the addition of only the laminate stiffnesses, which have been calculated reliably for a long time.



**FIGURE 17. FIBER PATTERNS TO AVOID PREMATURE MATRIX FAILURES IN UNNOTCHED CROSS-PLYED CARBON-EPOXY COMPOSITE LAMINATES**

It may appear that the author has made precisely the same mistake that he criticized others for; that is homogenizing the fibers and matrix into a single orthotropic composite material. It is true that the material properties are expressed at the lamina level, but the new failure criterion is really a normalized expression of the failure of the fibers alone. Actually, one should perform micromechanical analyses of the lamina and its constituents to relate the Poisson contractions of the fibers to those of the lamina because the transverse strains of the fibers need not be the same as for the lamina. And it is possible that, when this is done, pure-shear failures will be found to lie slightly off the  $-45$ -degree line in Figure 7, but still on the *same* shear failure line as for fiber failure under longitudinal tension or compression.

However, in the context of Figure 15, if the longitudinal Poisson's ratios of the fiber and lamina differed significantly, an *equivalent* failure envelope could be prepared for the Poisson's ratio of the fiber. There would be a compensatory shift in the location of the uniaxial failure points, but the *form* of the failure envelope would not change at all because the transverse strains were expressed at the lamina rather than fiber level. (Obviously, the longitudinal strains must be the same except for edge effects not normally addressed by laminate analysis.) Nevertheless, this simplification is appropriate *only* for those laminate patterns that are associated with fiber-dominated failures. The precise two-phase analysis would be required for matrix-dominated failures.

As is explained later, in order to superimpose fiber and matrix failure criteria, it is first necessary to use a common strain base — that of the laminate and hence of each lamina — rather than the strains of

the constituents. So, the failure envelopes should always be expressed at the lamina rather than constituent level. The net effect of a micromechanics analysis distinguishing between constituent and macro-strains would then appear as a change in slope of the line relating longitudinal to transverse strains within each lamina. The Poisson's ratio slopes given by  $\nu_{LT}$  and  $\nu_{TL}$  in Figure 7 would not change, but those defined by  $\nu_{xy}$  and  $\nu_{yx}$  in Figures 12 and 14 could. Likewise, the pure-shear point at the laminate level might not be precisely on the  $-45^\circ$  sloping line when assessed from the point of view of either the fiber or matrix.

### EFFECTS OF IN-PLANE SHEAR ON THE "LAMINA" FAILURE CRITERION

If the principal directions of stress or strain do not coincide with the fiber axes, a question arises as to the validity of the preceding failure criteria that makes no provision for such a situation. In the case of ductile *homogeneous* materials, the maximum-shear-stress failure (or yield) criterion in Figure 5 can *always* be used by a simple rotation of reference axes to coincide with the principal stress and strain directions, so this criterion is inherently complete. However, for fibrous composites, such a rotation of reference axes would invalidate the use of the simple stress-strain relations in Equations (19) through (21). Many more terms would then be needed to characterize the stress-strain relations. And the seemingly simple alternative of computing separate principal strains, applying them to the fiber directions instead of the real strains, would be incorrect in such a case.

Fortunately, a simple physically realistic resolution of this problem is available for the cases of most common interest in which stiff strong fibers are embedded in soft matrices. It is apparent that any shear stresses with respect to the fiber axes can cause neither longitudinal nor transverse stresses between those same axes. The principal effect of such shear stresses is to cause longitudinal and transverse direct stresses in those fibers inclined at  $45^\circ$  to the fibers under consideration. Such an effect is easily accounted for when checking the strength of those other fibers under a combination of only axial and transverse loads. Likewise, any shear between axes inclined at  $\pm 45^\circ$  with respect to the ( $0^\circ$ ) reference fibers is accounted for in the form of direct longitudinal and transverse stresses in the  $0^\circ$  and  $90^\circ$  fibers.

Nevertheless, the "minor" effect of the shear deformation is of potential concern. If the composite were truly homogeneous, both the fibers and the matrix would undergo the same shear strain in addition to any direct longitudinal and transverse strains. It would not be permissible to ignore the effects of such shear strains on the strength of the fibers. However, when the matrix is much softer than the fibers, most of the shear strain will be confined to the (resin) matrix and the fibers will not experience significant shear stresses. In such a case, it is reasonable to complete the "lamina" characteristic in the form shown in Figure 18. The in-plane shear strain cutoff shown for  $0^\circ/90^\circ$  shear on the resin matrix would normally be truncated by prior failure of the  $\pm 45^\circ$  fibers carrying the shear load. However, there would be no difficulty in applying the matrix shear strain as the dominant limit for very brittle matrices.

Unless there is a compelling reason to do otherwise, it is recommended here that the minor in-plane shear effects be ignored and consideration be given only to the associated direct loads in the  $\pm 45^\circ$  fibers and possibly the matrix-dominated  $0^\circ/90^\circ$  strength under those shear loads. Materials for which this simplification is reasonable include carbon, fiberglass and boron reinforced organic matrices like the epoxies.

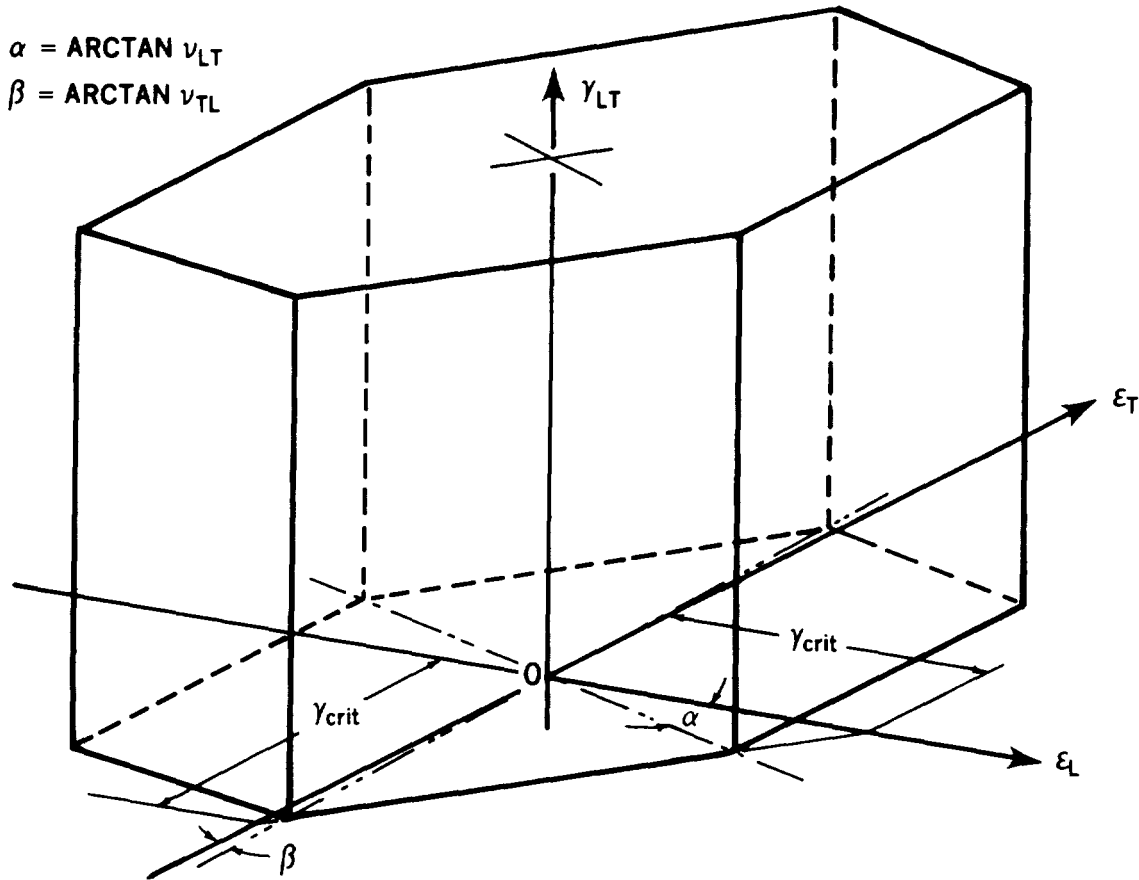
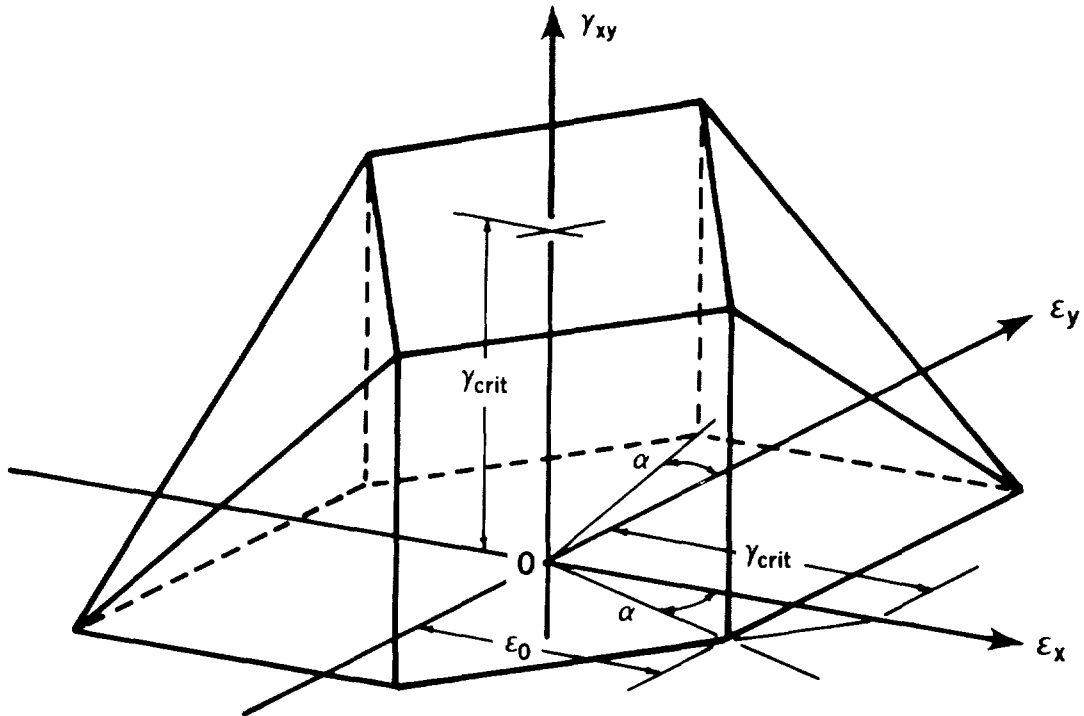


FIGURE 18. STRAIN-BASED LAMINA FAILURE CRITERION

Although Figure 18 refers to each individual lamina within the laminate, it is possible to deduce a universal failure envelope for any membrane state of stress (as opposed to bending) in any cross-plyed laminate containing two axes of material symmetry. This means that the percentages of the  $0^\circ$  and  $90^\circ$  plies may differ but that there must be the same number of  $+45^\circ$  plies as  $-45^\circ$  plies. Such a failure envelope is illustrated in Figure 19. It should be noted that this figure may be applied only with respect to the  $0^\circ$  and  $90^\circ$  axes, not with respect to the  $\pm 45^\circ$  axes. The single application of this form of failure criterion, however, encompasses all *four* fiber directions. Failure of either a  $0^\circ$  or  $90^\circ$  fiber occurs on the vertical "walls" of the failure envelope, while failure of the  $+45^\circ$  or  $-45^\circ$  fibers is predicted to occur somewhere on the roof. The zero-shear-strain ( $\epsilon_x - \epsilon_y$ ) plane is easily understood because it is taken directly from Figure 11. The height of the shear-strain plateau, likewise, follows from Figure 11, which shows that the equal and opposite direct strains in the  $\pm 45^\circ$  fibers then have a magnitude of  $\gamma_{crit}/2$ .

The size of the plateau in Figure 19 can be established by examining the strains in the  $+45^\circ$  and  $-45^\circ$  fibers at the points of uniaxial load. As shown in References 2 and 4, the strain in those fibers is less than in the  $0^\circ$  fibers, in the ratio of  $(1 - \nu)/2$  to 1. That would leave a longitudinal strain capacity of  $[(1 + \nu)/2]\epsilon = \gamma_{crit}/2$  to resist any simultaneously applied in-plane shear load. This is sufficient to accommodate an in-plane shear strain of precisely  $\gamma_{crit}$  with respect to the  $0^\circ/90^\circ$  fiber axes. The  $\pm 45^\circ$  fibers are critical in the  $L-N$  and  $T-N$  planes for this combination of  $0^\circ$  uniaxial tension and  $0^\circ/90^\circ$  shear. The  $L-T$  plane is not critical because the associated in-plane strain perpendicular to the more



$$\alpha = \text{ARCTAN } \nu_{LT} \text{ FOR UNIDIRECTIONAL LAMINA}$$

**FIGURE 19. UNIVERSAL STRAIN-BASED LAMINATE FAILURE CRITERION**

highly loaded fiber has the same sign as the axial strain. Since the governing Poisson's ratio is for the unidirectional lamina, this result applies for *all* cross-plyed laminates, regardless of their particular Poisson's ratios. (Obviously, for this combination of loads, only one of the  $\pm 45^\circ$  fiber directions will be critical, not both).

Of course, there is no shear strength capacity at the points of biaxial tension or compression in the  $\epsilon_x - \epsilon_y$  plane because *all* fibers are equally and fully strained there. The shear strength capacity varies linearly between those corner points and the edge of the shear strength plateau.

The applicability of Figure 19 to all cross-plyed fiber patterns with the same percentages of  $+45^\circ$  and  $-45^\circ$  plies is the reason why, in Figure 21 of Reference 4, the edges of the shear stress plateaus were at the same location for all three fiber patterns considered;  $0^\circ/90^\circ$ ,  $\pm 45^\circ$ , and quasi-isotropic.

While Figure 19 encompasses the great majority of failure envelopes for typical fibrous composites, there appears to be no justification for making similar simplifications for Kevlar (aramid) fibers that are weak in transverse shear or for metal-matrix or carbon-carbon composites with relatively stiff matrices. It would appear that the use of the maximum shear strain calculated from Mohr circles would then be more appropriate as a lower bound estimate of the failure of the fibers. However, this technique is complicated because the maximum shear strain could occur either in the  $L-T$  or  $L-N$  plane, or possibly in some other plane altogether, depending on the combination of applied loads. Moreover, not all shear strains in orthotropic materials are associated with any stresses (as is discussed later), and it is the stresses, not the strains, that cause failure of the material.

\* (Figure 20 is shown on the following page.)

The author advises caution in applying *any* simplified failure criteria to the more exotic composites under investigation today, and reminds the readers again that the very useful simple methods presented here should be applied only to conventional fibrous composites such as carbon epoxies, in which strong, stiff fibers are embedded in relatively soft matrices.

### EXPERIMENTAL VERIFICATION

The author's research into predicting the strength of cross-plyed composite laminates was motivated by the development over 15 years ago of a reliable in-plane shear test specimen, shown in Figure 20. The laminate strengths achieved on that specimen, which were twice as high as had been obtained on more customary contemporary shear test coupons, were still only about half as high as predicted by contemporary failure criteria. Almost another decade passed before the author could determine what was wrong with those theories. With a fuller understanding of the subject, it became apparent that unidirectionally loaded test coupons were so completely dominated by the behavior of fibers aligned in the same direction as the load that they could never invalidate faulty strength-prediction theories. Only biaxial tests were sufficiently sensitive to other properties as well to be able to validate theories. Accordingly, the author prepared a series of papers on biaxial test specimens (see References 5 through 7) to make it possible to discriminate between failure theories that were suitable for fibrous composites and those that were not.

Fortunately, other researchers felt the same way. Swanson, in particular, generated biaxial test data on carefully fabricated and tested pressurized axially loaded tubes. The results of Swanson and his

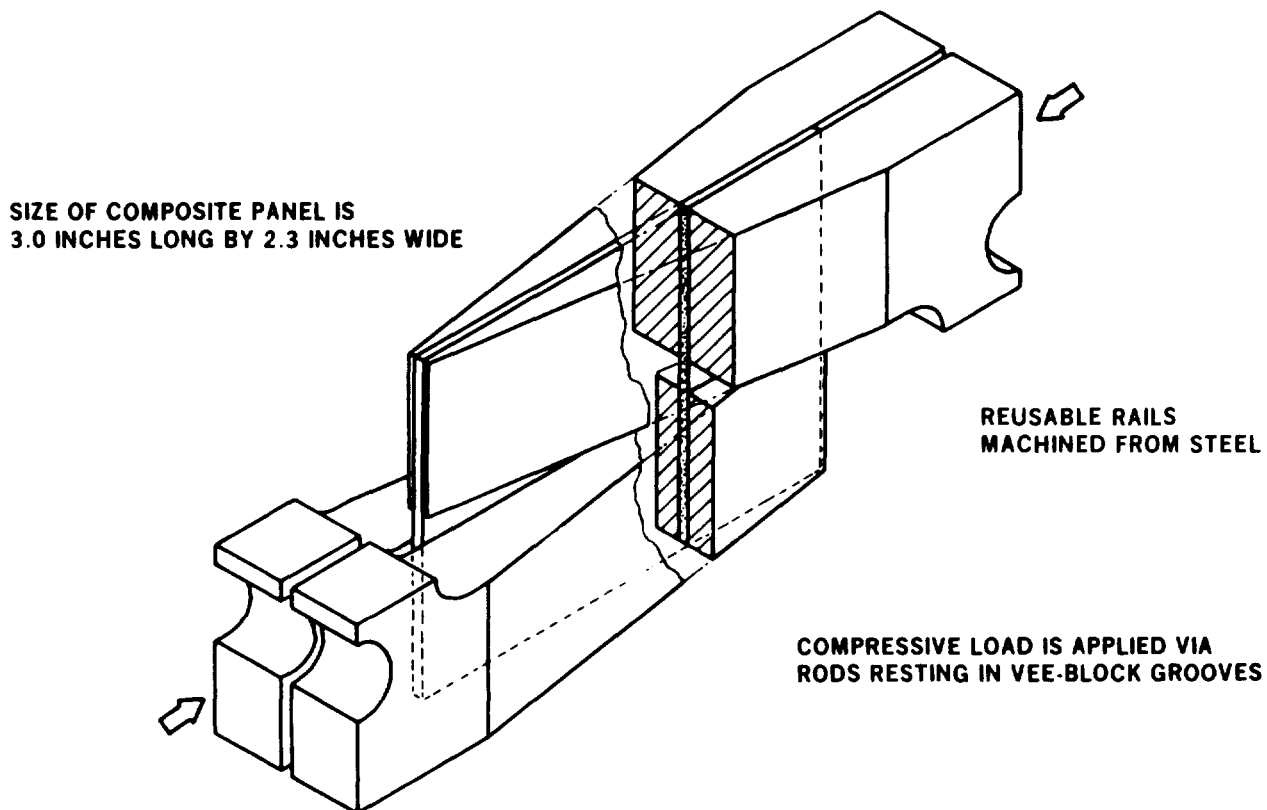
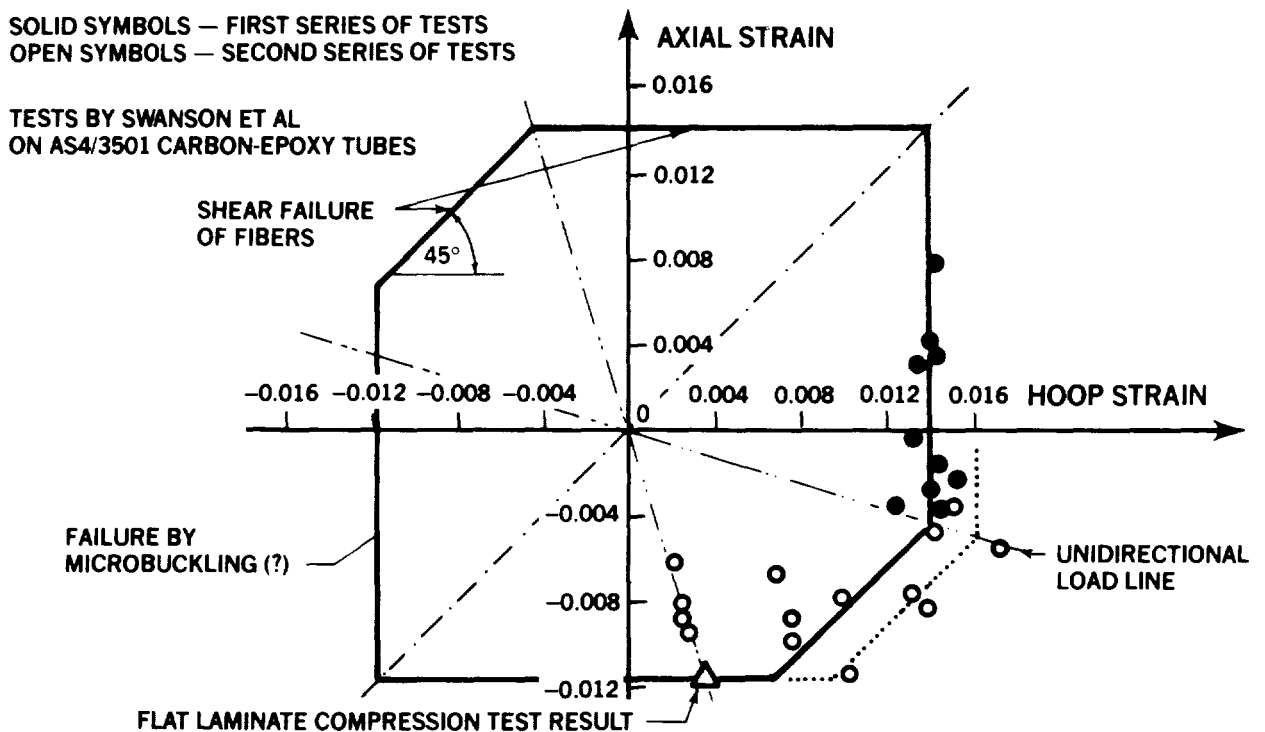


FIGURE 20. DOUGLAS BONDED, TAPERED RAIL-SHEAR TEST SPECIMEN

co-workers (Reference 8) are reproduced here in Figure 21 and compared with the present theory. The agreement is obviously excellent for the tension-tension biaxial loads, covered by the first series of tests and identified by the solid symbols.

However, the author suspects that the second batch of tubes were either made with more precision or of stronger material since the open symbols display a higher strength at the uniaxial hoop load point. The predicted shear failures, based on the earlier tensile strengths, seem to be premature, but would agree well if the 45-degree sloping lines were moved outward to pass through the higher unidirectional strain-to-failure for the later tests (identified by the open symbols). It was obvious to Swanson and his colleagues that the predominantly compressively loaded specimens were failing prematurely, even though they were unable to find reasons for this.



**FIGURE 21. COMPARISON BETWEEN TEST AND THEORY FOR TRUNCATED MAXIMUM-STRAIN FAILURE MODEL FOR CARBON-EPOXY COMPOSITES**

The predicted compressive strengths shown in Figure 21 are based on the unidirectional compressive strain-to-failure cited by Swanson but, even so, the tubes failed at a still lower strain. Some, but not all, of the most premature failures were associated with compression of the thinnest tubes tested. Even when all these premature failures are explained, it is likely that the cause would recur in real structures subject to the same kind of loading, submersible vehicles, for example.

It is evident that some mechanism other than shear failures of the fibers must have governed those compression failures. However, as shown in Figure 15, the present theory makes provision for such a possibility, and it is not at all difficult to add a cut-off representing a different compressive failure mode in part of a predominantly shear-failure envelope. Indeed, Figure 21 makes such a distinction.

Unfortunately, tests of biaxially loaded composite specimens are often conducted without analysis of probable failure modes and strengths, and most of these data are generally regarded as unreliable.



Therefore, such tests failed to influence researchers developing composite failure criteria. And, since the far more numerous uniaxially loaded test specimens were incapable of exposing defective theories, analytical improvements were not forthcoming. Indeed, as explained in Reference 9, none of the standard test coupons, with one exception, the tension test of a  $\pm 45^\circ$  laminate, could even be relied upon to generate reliable lamina data from which to calculate the strength of cross-ply laminates.

However, since the standard composite failure theories were incapable of making consistently correct predictions, even if they were given good input properties, such shortcomings of the standard test specimens were not as bad as they seemed at first sight. Composite designs are customarily carried out at reduced strain allowables to allow for stress concentrations at bolt holes and for damage tolerance. Barely 1 percent of typical commercial aircraft composite structures are sized by unnotched allowable strengths.

### A BROADER PERSPECTIVE

As shown in this paper, a failure criterion can be based on a single shear *strain* allowable if hygro-thermal strains that do not cause any stresses are eliminated from consideration. Shear strains induced by Poisson contractions in the absence of any shear stress must also be eliminated. There is no counterpart of this phenomenon for isotropic materials that have only one Poisson's ratio. However, for materials having different Poisson's ratios with respect to different material reference axes, the presence of strain in the absence of equivalent stress is quite possible. Heating an unrestrained homogeneous isotropic material cannot create either shear stresses or strains. For an orthotropic material, on the other hand, if the coefficient of thermal expansion varies with orientation, the principal thermally induced strains will differ so that shear strains must be developed. However, since the orthotropic object is presumed to be unrestrained while being heated, there can be no stresses. In a strict mathematical sense, this phenomenon and the equivalent one involving Poisson contractions are covered by assigning the value zero to the appropriate coefficients in the thermo-elastic relations.

In the absence of applied normal stresses, an axial load in a unidirectional lamina will cause the same Poisson contractions in both the transverse and normal directions. Therefore this load cannot possibly contribute to any shear strains in the plane of isotropy perpendicular to the fiber axes. This is confirmed by rearranging Equations (20) and (21) for transversely isotropic materials to express the difference between normal and transverse contractions for any combination of axial and transverse loads. It is found that

$$\epsilon_T - \epsilon_N = (1 + \nu_{TN})\sigma_T/E_T \quad (24)$$

no matter what longitudinal stress is applied.

The corresponding principal strain differences between the other pairs of axes follow similarly from Equations (19) to (21). First,

$$\epsilon_L - \epsilon_N = \left( \frac{1 + \nu_{LT}}{E_L} \right) \sigma_L + \left( \frac{\nu_{TN} - \nu_{TL}}{E_T} \right) \sigma_T \quad (25)$$

in which the second term cannot contribute to the stresses in the L-N plane and must therefore be omitted from the failure criterion. Finally,

$$\epsilon_L - \epsilon_T = \left( \frac{1 + \nu_{LT}}{E_L} \right) \sigma_L - \left( \frac{1 + \nu_{TL}}{E_T} \right) \sigma_T \quad (26)$$

in which *both* terms contribute fully to the stresses in the L-T plane, but the first has no effect on the T-N plane.

With reference to Figure 15, the 45-degree sloping lines are defined by both terms in Equation (26) while the vertical lines are defined by the first term on the right side of Equation (25) and the horizontal lines are defined by the mirror images of the vertical lines. Equation (24) is assumed here not to be a governing strength limit for strong, stiff fibers in a soft matrix.

The general theory of elasticity for anisotropic materials could probably be applied to reduce the failure criterion to an unambiguous state without needing logic to drop certain terms from the simpler formulation given here. However, the end result should be the same for fiber-dominated failures of the composite materials considered here, but this approach might be incredibly complex.

What concerns the author most is not good designs in today's composite materials; it is the identification of impractical fiber patterns that lead to weak structures with matrix-dominated failures. Fiber-dominated failures can be analyzed using a theory as simple as the present one. The more complex theories accounting properly for matrix-dominated failures are needed only to identify fiber patterns that should not be used and for which, therefore, there should be no need to predict the strengths. There is also a concern that the present theory is probably inadequate for the more exotic composite materials of the future. It is time to stop pretending that there is a scientific validity to the majority of the methods used to predict the strength of fibrous composite materials, no matter how elegant the mathematics, and it is time to acknowledge the need for much new work on a secure foundation. There are opportunities for tremendous contributions to this field, provided that they have the scientific realism needed for such analyses.

Since the presentation of his first papers on composite failure theory (References 2 and 3) the author has been progressively deriving various pieces of the theory needed for a completely rigorous two-phase composite strength-prediction theory. The intent had been that, on its completion, that work would be simplified for the customary fibrous composites in use today and any approximations made would be justified by comparison with the more general theory. As fate would have it, the second step has been completed first. Nevertheless, a summary of certain features of the more precise analyses, may help to guide future researchers.

Figure 22 indicates the features needing to be included in a proper two-constituent (phase) characterization of the strength of cross-plyed fibrous composite laminates. One or the other envelope may dominate, depending on the particular state of stress. And, although the shear-strain plateaus are not shown, the same consideration of one or the other being dominant is just as applicable as for the interaction between the direct in-plane loads.

In order that the individual failure envelopes for each constituent (or phase) of the composite material may be superimposed as shown, all strains must be expressed at some common level, for example, that

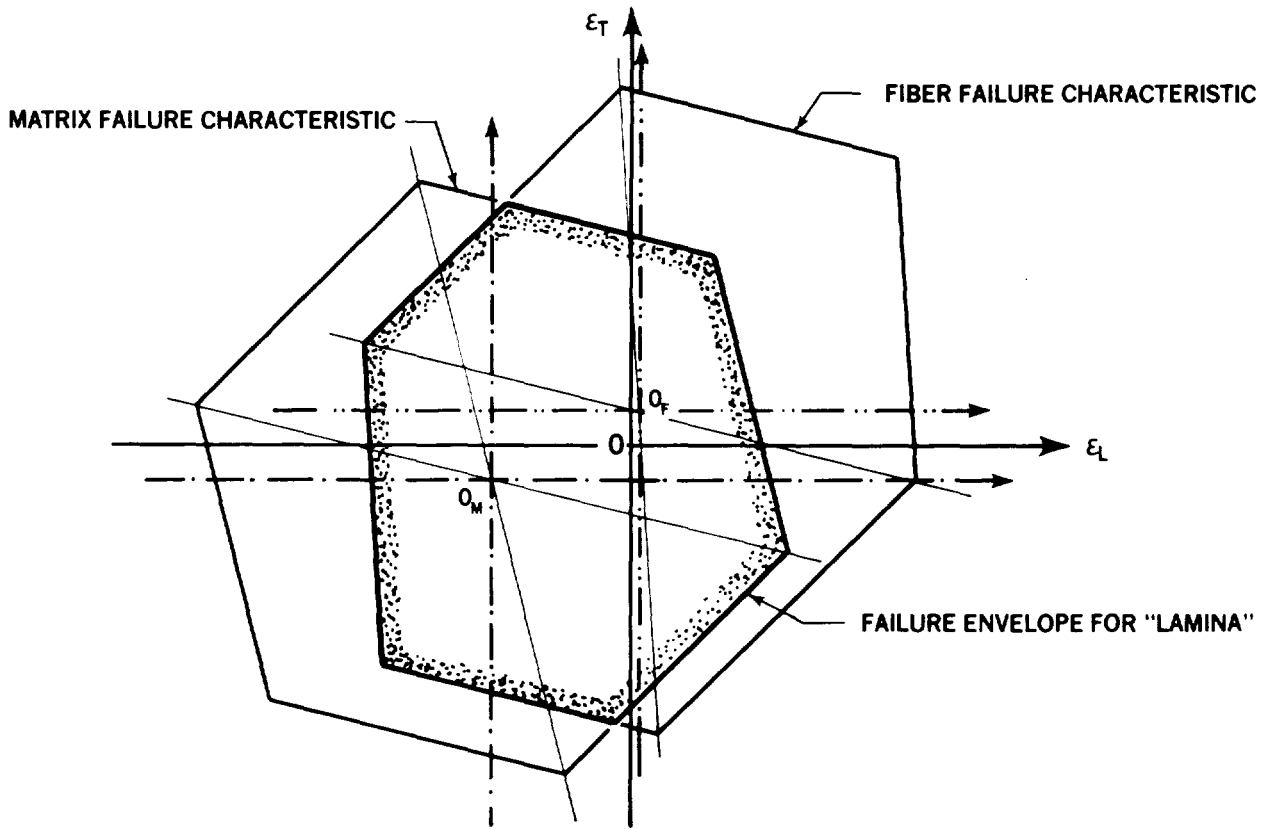


**FIGURE 22. SEPARATE FAILURE CHARACTERISTICS FOR FIBERS AND MATRIX**

of the lamina rather than at the constituent level. For example, longitudinal strains parallel to fibers are inevitably the same for both fibers and matrix, except for a minute edge zone. On the other hand, the strains perpendicular to the fibers need not be common and are usually not. Therefore, the fiber failure characteristic in Figure 22 could appear to have a different Poisson's ratio than an isolated fiber, for example. Likewise, for the resin matrix in which the transverse strains vary considerably because of the fibrous "inclusions," the transverse strains in Figure 22 would have to be averaged over a small but finite distance. The "failure" strain shown would correspond to some different strain at the microscopic level that was actually associated with the stress at which failure occurred.

This difference between constituent and equivalent "lamina" behavior is explained in Figure 23, where there are two shear failure lines drawn for the fiber failure envelope. The fiber is presumed to have a higher transverse stiffness than the resin matrix so, for a common axial strain under a unidirectional load, two different lateral contractions (corresponding to two different Poisson's ratios) are established. It is, of course, the same failure characteristic, but it can be superimposed on matrix failures in only one form. Figure 23 shows also the corresponding locations of the pure in-plane shear failure locations. It is apparent that, in this case, the blind use of the "lamina" rather than the "fiber" Poisson's ratio would result in an underestimate of the axial strain in the fiber at which in-plane shear failure occurred. (But the converse could happen for titanium-matrix composites, for example.)

Figure 23 is not only designed to explain how the generalization of the classical maximum-shear-stress failure criterion can still be applied in combination with micromechanics analysis for the more exotic composite materials, but to reinforce the suggestion that there is no need to go to such lengths for

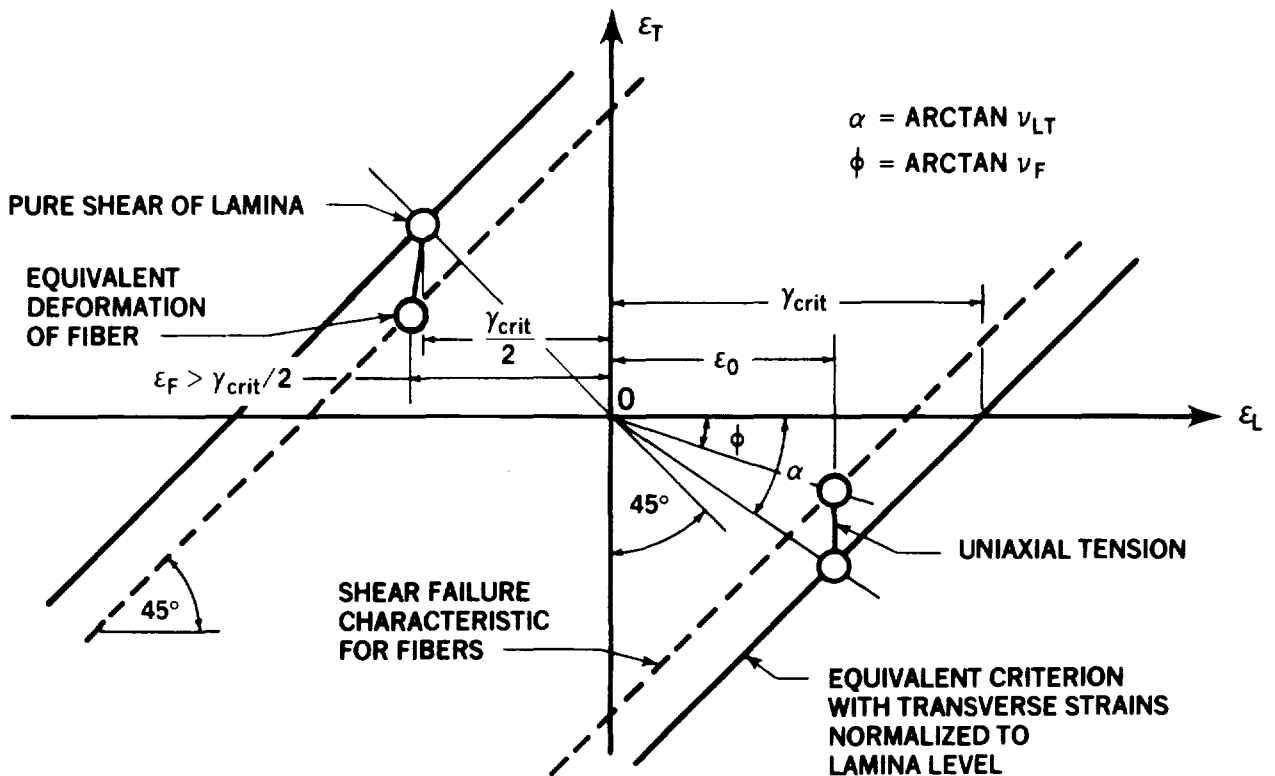


FIGURE 23. EQUIVALENT SHEAR FAILURE CRITERIA AT FIBER AND LAMINA LEVEL

conventional fiber/resin composites in which the differences between the Poisson contractions of the fiber and lamina are small enough to be neglected.

The shape of the individual failure envelopes in Figure 22 for the fibers and matrix could change with the operating temperature. Similarly, there could be a shift in the origins  $O_F$  and  $O_M$  which are offset appropriately to allow for residual thermal stresses in each constituent from curing at an elevated temperature and operating the structure at high temperatures, where it is very cold. The amount of shift between the origins can be computed on the basis of micromechanical analysis, as in Reference 10. Since the origin shifts and the matrix failure envelope would vary with operating temperature, the form of the overlapping region of the individual failure envelopes would correspondingly change with service temperature as well. Such an effect cannot be accounted for in any homogenized model supposedly characterizing any composite material.

There is no evidence to suggest that these residual thermal stresses can creep out and relieve themselves significantly. When the residual stress intensity is high at room temperature or below, the matrix is highly resistant to creep. And, when the creep resistance is reduced at elevated temperatures, so are the stresses that would cause the creep. Moreover, the suggestion that the residual thermal stresses can be nullified by swelling stresses due to moisture absorption, merely clouds the issue by making the stress-free temperature vary with the manufacturing and service history for each particular structure. In any event, the rate of diffusion is typically so slow that reliance on any absorbed moisture to relieve curing stresses would in turn introduce the problem of how to treat the effects of that water during a rapid change in temperature.

It should be noted that the residual stresses are definitely *not* a lamina property. Most prior treatments of residual thermal stresses have started with the false premise that the individual lamina is homogeneous and inherently stress-free in isolation, no matter what its temperature. Such an oversimplification cannot possibly explain matrix cracking. It is even questionable for use in characterizing edge delaminations resulting from stacking together too many parallel layers of unidirectional material, whether these delaminations be caused by thermal or mechanical stresses. It was actually these edge-delamination stresses that led to the outer fiber-pattern limits in Figure 17 (for typical carbon-epoxy composites), so there are really *three* potential failure modes to consider for typical fibrous composite laminates.

Matrix failures, either intraply or interply, *always* represent an inability to develop the full strength of the fibers and should therefore be avoided by choice of an appropriate fiber pattern and layer sequence for each laminate. Mathematical composite failure theories have not adequately addressed matrix failures and, until they do, one should use good judgment to exclude the inferior arrangements rather than believe that such constraints do not exist merely because one's computer program is not smart enough to advise users of its weaknesses. Actually, far more restrictive limits on fiber patterns arise when one considers bolt holes, which introduce even further matrix-dominated influences on the degree of stress-concentration relief, as shown by the inner fiber pattern limits in Figure 17. The author believes that matrix-dominated failures will continue to require empiricism even after rigorous two-phase theories have been developed for unnotched laminates. So, the use of a simple failure model that adequately characterizes only fiber-dominated failures can be just as reliable as more elaborate theories, provided that it is used in conjunction with realistic constraints on fiber patterns.

## IMPLEMENTATION OF MAXIMUM-SHEAR-STRESS FAILURE CRITERION FOR FIBROUS COMPOSITE LAMINATES

---

### TESTS:

#### RECORD COMPLETE LOAD-DEFLECTION CHARACTERISTICS:

1.  $0^\circ$  LAMINATE — MODULUS AND POISSON'S RATIO
2.  $0^\circ/90^\circ$  LAMINATE — MODULUS, TENSILE AND COMPRESSIVE STRENGTHS, AND STRAINS TO FAILURE
3.  $\pm 45^\circ$  LAMINATE — MODULUS, POISSON'S RATIO, AND TENSILE STRENGTH

### UNIDIRECTIONAL (ALL $0^\circ$ ) LAMINA PROPERTIES:

#### WOVEN FABRICS SHOULD BE CONSIDERED A COMBINATION OF TAPE LAYERS:

1. LONGITUDINAL MODULUS  $E_L$  — FROM TEST 1
2. TRANSVERSE MODULUS  $E_T$  — FROM DIFFERENCES BETWEEN TESTS 1 AND 2
3. LONGITUDINAL POISSON'S RATIO  $\nu_{LT}$  — FROM TEST 1 (OR DEDUCED FROM TEST 3 FOR WOVEN FABRICS)
4. IN-PLANE SHEAR MODULUS  $G_{LT}$  — FROM TEST 3
5. LONGITUDINAL TENSILE AND COMPRESSIVE MONOLAYER STRENGTHS  $F_L^u$  AND  $F_L^c$  (OR STRAINS TO FAILURE) — DETERMINED FROM TEST 2 USING PROPERTIES 1 AND 2
6. IN-PLANE SHEAR STRENGTH  $F_{LT}^u$  — FROM TEST 3
7. TRANSVERSE STRENGTH  $F_T^u$  — IRRELEVANT FOR CROSS-PLYED STRUCTURAL LAMINATES OF TYPICAL FIBER/POLYMER COMPOSITES

### APPLICATION:

CHECK COMBINATION OF LONGITUDINAL AND TRANSVERSE STRAINS FOR EACH FIBER DIRECTION OR FOR ORTHOGONAL SETS OF FIBERS

---

## CONCLUSIONS

A simple and physically realistic method for predicting the strength of cross-plyed fibrous composite laminates has been shown here to follow from a generalization of the classical maximum-shear-stress yield criterion for ductile metal alloys.

The generalization to orthotropic materials has required that the failure criterion be expressed in terms of strains rather than the more customary stresses, even though the actual governing criterion is one of stress.

The new failure criterion is shown to be similar to a simple truncation in the in-plane shear quadrants of the well-known maximum-strain empirical failure model for composites. Therefore, this new work is closely related to the best known classical failure models for both ductile metals and composite laminates. The new theory has also been compared favorably with biaxial test data of other researchers.

While the new theory is unlikely to be improved upon for state-of-the-art fiber/polymer composites, there remains a need for a proper two-phase strength analysis. Separate accounting for failures in the fiber or in the matrix will be needed both for matrix-dominated failures in impractical fiber patterns with today's composites and for predicting any failures of the more exotic composites that are as yet only in the research and early applications stage.

## ACKNOWLEDGMENT

Two of the author's colleagues at Douglas have contributed significantly to this work. Dave Peterson coded the BLACKART computer program used to assess the effects of all the usual input on the output from composite strength-prediction methods. Benson Black was the first to recognize that the failure of *all* cross-plyed laminates could be reduced to a *single* shear-failure characteristic regardless of the fiber pattern. Even without the benefit of this latest research, the empirical shear cutoffs he applied to the use of the maximum-strain failure criterion for C-17 composite components are remarkably close to the best recommendations that could be made today. The information presented here would have taken much longer to develop without such support and advice.

The author would also like to acknowledge the encouragement from the MIL-HDBK-17 committee members and, in particular, the U.S. Army MTL and FAA representatives to persevere with this work.

## REFERENCES

1. Waddoups, M. E., "Characterization and Design of Composite Materials," in *Composite Materials Workshop*, edited by S. W. Tsai, J. C. Halpin, and N. J. Paganó, Technomic, Connecticut (1968), pp. 254-308.
2. Hart-Smith, L. J., "Simplified Estimation of Stiffness and Biaxial Strengths for Design of Laminated Carbon-Epoxy Composite Structures," Douglas Aircraft Company, Paper 7548, unlimited distribution. Presented to Seventh DoD/NASA Conference on Fibrous Composites in Structural Design, Denver, Colorado, June 17-20, 1985; published in Proceedings, AFWAL-TR-85-3094, pp. V(a)-17 to V(a)-52.

3. Hart-Smith, L. J., "Simplified Estimation of Stiffnesses and Biaxial Strengths of Woven Carbon-Epoxy Composites," Douglas Aircraft Company, Paper 7632, unlimited distribution. Presented to 31st National SAMPE Symposium and Exhibition, Las Vegas, Nevada, April 7-10, 1986; published in Closed-Session Proceedings, pp. 83-102.
4. Peterson, D. A., and Hart-Smith, L. J., "A Rational Development of Lamina-to-Laminate Analysis Methods for Fibrous Composites," Douglas Aircraft Company, Paper 7928, presented to 9th ASTM Symposium on Composite Materials: Testing and Design, Sparks, Nevada, April 27-29, 1988; to be published in ASTM STP 1059.
5. Black, J. B. Jr., and Hart-Smith, L. J., "The Douglas Bonded Tapered Rail-Shear Test Specimen for Fibrous Composite Laminates," Douglas Aircraft Company, Paper 7764, presented to 32nd International SAMPE Symposium and Exhibition, Anaheim, California, April 6-9, 1987; published in Proceedings, pp. 360-372.
6. Hart-Smith, L. J., "A Radical Proposal for In-Plane Shear Testing of Fibrous Composite Laminates," Douglas Aircraft Company, Paper 7761, presented to 32nd International SAMPE Symposium and Exhibition, Anaheim, California, April 6-9, 1987; published in Proceedings, pp. 349-359.
7. Hart-Smith, L. J., "A Biaxial Test for Composite Laminates Using Circular Honeycomb Sandwich Panels," Douglas Aircraft Company, Paper 7974, presented to 33rd International SAMPE Symposium and Exhibition, Anaheim, California, March 7-10, 1988; published in Proceedings, pp. 1485-1498.
8. Swanson, S. R., and Nelson, M., "Failure Properties of Carbon/Epoxy Laminates under Tension-Compression Biaxial Stress," in *Composites '86: Recent Advances in Japan and the United States*, edited by K. Kawata, S. Umekawa, and A. Koyabashi, Proceedings of the Third Japan-U.S. Conference on Composite Materials, Tokyo, Japan, June 23-25, 1986, pp. 279-286.
9. Hart-Smith, L. J., "Some Observations About Test Specimens and Structural Analysis for Fibrous Composites," Douglas Aircraft Company, Paper 7929, presented to 9th ASTM Symposium on Composite Materials: Testing and Design, Sparks, Nevada, April 27-29, 1988; to be published in ASTM STP 1059.
10. Hart-Smith, L. J. "A Simple Two-Phase Theory for Thermal Stresses in Cross-Plied Composite Laminates," Douglas Aircraft Company, Report MDC K0337, December 1986.